MICROBIAL SEDIMENTOLOGY OF STROMATOLITES IN NEOPROTEROZOIC CAP CARBONATES

TANJA BOSAK[1], GIULIO MARIOTTI[2], FRANCIS A. MACDONALD[3], J. TAYLOR PERRON[4], AND SARA B. PRUSS[5]

[1]E25-649, Department of Earth, Atmospheric and Planetary Sciences, MIT, Cambridge, MA 02139 USA <tbosak@mit.edu>

[2]54-827, Department of Earth, Atmospheric and Planetary Sciences, MIT, Cambridge, MA 02139 USA

[3]20 Oxford Street, Department of Earth and Planetary Science, Harvard University, Cambridge, MA 02138 USA

[4]54-1022, Department of Earth, Atmospheric and Planetary Sciences, MIT, Cambridge, MA 02139 USA

[5]The Department of Geosciences, Clark Science Center, Smith College, Northampton, MA 01063 USA

ABSTRACT.—Stromatolite shapes, sizes, and spacings are products of microbial processes and interactions with topography, sedimentation, and flow. Laboratory experiments and studies of modern microbial mats and sediments can help reconstruct processes that shaped some typical stromatolite forms and some atypical microbially influenced sediments from Neoproterozoic cap carbonates. Studies of modern, cohesive microbial mats indicate that microbialaminite facies in the lower Rasthof Formation (Cryogenian) formed in the presence of very low flow and were not deformed by strong waves or currents. Giant wave ripples, corrugated stromatolites, and tube-hosting stromatolites in basal Ediacaran cap carbonates record interactions between microbes, flow, and evolving bedforms. Preferential cementation in and close to the giant ripple crests is attributed to interactions between flow and local topography. These interactions pumped alkaline porewaters into ripple crests and helped nucleate elongated stromatolites. The similar textures of giant wave ripples and elongated, corrugated, and tube-hosting stromatolites suggest growth in the presence of organic-rich, rounded particles and microbial mats, and in flow regimes that permitted mat growth. These hypotheses can be tested by experiments and models that investigate lithification and the macroscopic morphology of microbial mats as a function of the flow regime, preexisting topography, redox-stratification in sediments, and delivery of organic-rich particles. The widespread microbially influenced textures in Cryogenian microbialaminites and basal Ediacaran cap dolostones record a strong reliance of carbonate deposition on the presence of organic nuclei, supporting carbonate accumulation rates comparable to those in modern reefs. Therefore, the unusual macroscopic morphologies of microbially influenced facies in Neoproterozoic cap carbonates may not reflect oceans that were greatly oversaturated with respect to carbonate minerals.

INTRODUCTION

Modern aquatic environments abound with microbial twines and jellylike sticky substances that blanket mineral grains, interact with the moving sediments and fluids, and create hardgrounds. These macroscopic aggregates of microbes, extracellular polymeric substances (EPS), and, sometimes minerals, are known as microbial mats. Currents and evaporation in modern peritidal and intertidal environments can ripple, chip, fold, pit, dry out, or crack cohesive microbial mats (e.g., Horodyski et al., 1977; Gerdes et al., 2000; Noffke et al., 2001; Schieber et al., 2007). Enhanced mineral precipitation has preserved evidence of such microbially induced sedimentary structures (MISS) in shallow siliciclastic environments since the Archean (e.g., Noffke, 2010). Microbially stabilized sediments also were common in sub-wave base siliciclastic

In *Ecosystem Paleobiology and Geobiology*, *The Paleontological Society Short Course, October 26, 2013. The Paleontological Society Papers, Volume 19, Andrew M. Bush, Sara B. Pruss, and Jonathan L. Payne (eds.).*

environments during the Ediacaran (e.g., Gehling, 2000). Microbial mats in carbonate depositional environments have an extensive fossil record that extends from the peritidal into the subtidal realm due to microbially enhanced sediment stabilization by EPS (Paterson, 1997) or enmeshing filaments (e.g., Black, 1933; Ginsburg and Lowenstam, 1958; Gebelein, 1969; Neumann et al., 1970; Scoffin, 1970; Reid et al., 2000), and precipitation of carbonate minerals on organic surfaces (e.g., Trichet and Défarge, 1995; Riding, 2000; Dupraz et al., 2009). These processes may have built stromatolites—laminated and lithified sedimentary structures—since the early Archean (Hofmann, 2000; Schopf, 2006).

The shapes of modern marine stromatolites range from stratiform to dm- to m-sized clubs, ridges, cauliflower heads, or small domes (Logan et al., 1964; Gebelein, 1969; Playford, 1980; Burne and Moore, 1987; Spadafora et al., 2010). Stromatolites with much more diverse shapes and sizes were present during the Precambrian. These structures exhibited predictable forms on individual carbonate platforms (e.g., Hoffman, 1974; Horodyski, 1975; Grey and Thorne, 1985; Altermann, 2008), and likely tracked chemical, biological, and physical changes through time (e.g., Cloud and Semikhatov, 1969; Semikhatov et al., 1979; Walter and Heys, 1985; Awramik and Riding, 1988; Kah and Knoll, 1996; Semikhatov and Raaben, 1996; Knoll and Semikhatov, 1998; Grotzinger and Knoll, 1999; Raaben, 2006; Tice et al., 2011; Bosak et al., 2013). When biological, chemical, and physical regimes that contribute to stromatolite textures or shapes can be reconstructed, stromatolites can be used to recognize and interpret broader environmental and evolutionary trends. Models that consider realistic stromatolite-building processes on appropriate spatial and temporal scales are a necessary tool in these reconstructions (reviewed in Bosak et al., 2013).

Existing models of stromatolite morphogenesis explain how and why processes at the μm- to mm-scale produce individual laminae and textures, but have difficulty translating this into the observed diversity of stromatolite shapes at the cm- to m-scale. Commonly, diagenetic processes complicate these relationships even further by obliterating small-scale textural information. Current and past models and interpretations of stromatolite growth and form have relied on studies of sub-mm-scale laminae and textures (e.g., Hofmann, 1975; Monty, 1976; Burne and Moore, 1987; Knoll and Semikhatov, 1998; Seong-Joo et al., 2000; Seong-Joo and Golubic, 2000; Visscher et al., 2000; Sprachta et al., 2001; Vasconcelos et al., 2006; Bosak et al., 2009, 2010; Bontognali et al., 2010; Petryshyn and Corsetti, 2011; Mata et al., 2012), sub-mm or mm-scale angles of fossil biofilms and stromatolite laminae (Tice et al., 2011; Petroff et al., in press), mm-wide and tall tufts (Buick, 1992; Sim et al., 2012) or clumps in photosynthetic mats (Sim et al., 2012), and mm-scale laminae packed with trapped and bound grains (Black, 1933; Gebelein, 1969; Reid et al., 2003). A model that explores competition for nutrients in diffusion-limited mats accounts for the somewhat larger, cm-scale spacing of small conical stromatolites (Petroff et al., 2010). Another model that links mineralization in the mat to the distribution of the overlying biomass explains the observed relationship between the curvature and apical thickness recorded by the laminae of cm-scale and much larger conical stromatolites (Petroff et al., in press).

Morphogenetic models of dm-scale and larger columnar stromatolites invariably invoke the influence of currents, waves, and basin geometry (e.g., Gebelein, 1969; Hoffman, 1974; Eckman et al., 2008; Jahnert and Collins, 2012). For example, drawing on interpretations of modern analogs, m-scale stromatolite elongation perpendicular to the coastline is attributed to shore-perpendicular flows, whereas longshore currents or undocumented wind-induced circulation are thought to impart coastline-parallel elongation on stromatolites (Logan, 1961; Logan et al., 1964; Playford, 1980). In some cases, stromatolite elongation and inclination can additionally constrain the direction of sediment supply, particularly in stromatolites from littoral and sub-littoral areas with tidal currents (Gebelein, 1969; Hoffman, 1976). Modern marine stromatolites in the bights of Hamelin Pool are elongated normal to shoreline (Hoffman, 1976), suggesting the delivery of sediments by shoreline-normal flow. However, as-yet unknown factors organize these stromatolites into wide (>10 m) rows that are aligned approximately parallel to the shoreline (Playford and Cockbain, 1976; Playford, 1980). These uncertainties about stromatolite-shaping mechanisms, combined with the occasional lack of geological constraints as to the direction of the paleoshoreline, allow at least three interpretations of stromatolite elongation: 1) parallel to shore-normal currents, 2) parallel to

longshore currents, and 3) parallel to wind direction. Thus, paleoenvironmental interpretations can be ambiguous even in the case of common and conspicuous stromatolite forms that have modern analogs. Even more poorly understood are interactions among microbial growth, cementation, flow, and sediment transport over the evolving bed topography, although these may be responsible for most of the diversity among stromatolite forms (Bosak et al., 2013).

Stromatolites in cap carbonates, the m- to 100 m-thick carbonate sequences deposited in the aftermath of the two Neoproterozoic low-latitude glaciations, offer some of the most interesting interpretational challenges. Cap carbonates were deposited worldwide and are isotopically, petrographically, sedimentologically, and chemically distinct, suggesting formation in the presence of unusually high temperatures, high pCO_2 (Bao et al., 2008, 2009), glacioeustatic changes, and ice-sheet gravitational effects (Hoffman et al., 1998, 2007; Hoffman and Macdonald, 2010; Hoffman, 2011; see also for evidence for glaciations and conditions before, during, and after the glaciations). Cap carbonates have generated hypotheses about extreme carbonate sedimentation rates of meters to tens of m/1000 years (Hoffman et al., 2007), extreme weather (Allen and Hoffman, 2005), as well as density-stratified (Shields, 2005) and acidified oceans (Kasemann et al., 2005, 2010). Although the deposition of cap carbonate sequences followed both glaciations, the two sequences have distinct features that may reflect accretion in the presence of different chemical and physical conditions. The older Cryogenian cap carbonates tend to be relatively thin and dominated by limestone and dolostone, whereas the younger, basal Ediacaran cap carbonates consist of peloidal dolostone in microbially-influenced facies that form unusual stromatolite morphologies and high-relief bedforms (Hoffman and Schrag, 2002; Pruss et al., 2010; Hoffman, 2011).

In this paper, three examples of microbially-influenced facies in Neoproterozoic cap carbonates are discussed: convoluted micritic microbialaminites from the Cryogenian cap carbonates, and elongated and tubestone stromatolites from the basal Ediacaran cap carbonates. The main goals of this contribution are to: 1) highlight some gaps between the fossil record, modern analogs, and stromatolite growth models; 2) illustrate how microbial sedimentology can help reconstruct processes and environmental conditions that shaped stromatolites; and 3) present some testable hypotheses. Mechanisms responsible for the convolution in microbialaminites of the lower Rasthof Formation are discussed in light of mechanical properties of modern cohesive microbial mats, and patterns that arise when mats are disrupted at different flow regimes. The growth and disruption patterns in modern microbial mats bolster the interpretation that the laterally extensive Cryogenian microbialaminites were deposited below storm wave base (Pruss et al., 2010). Studies that explore the timescale of growth and lithification of modern textural analogs of Cryogenian microbialaminites yield estimates of carbonate deposition rates in the Cryogenian facies that are higher than 2–10 cm/kyr, which is comparable to, but not faster than, the accretion rates of modern shallow-water carbonates. Bedforms and stromatolites in basal Ediacaran cap carbonates stimulate new and testable hypotheses about stromatolite and bedform morphogenesis influenced by sediment, flow, redox-stratified sediments, and light organic particles. Studies of modern and ancient mats with peloidal textures suggest that stromatolitic facies in basal Ediacaran cap carbonates accreted at rates comparable to those in modern-day shallow-water carbonates and did not outpace biological growth rates. Therefore, textures and macroscopic morphologies of the Cryogenian and basal Ediacaran cap carbonates offer little evidence of highly oversaturated seawater and extraordinarily fast carbonate accumulation. Instead, they may record a very tight coupling between the rates of carbonate sedimentation and microbial growth in the presence of high pCO_2.

MICROBIAL STRUCTURES IN CRYOGENIAN CAP CARBONATES

Cap carbonates deposited in the aftermath of the two Neoproterozoic low-latitude glaciations (Snowball Earth events; Hoffman and Schrag, 2002) contain stromatolite forms that have puzzled geologists for decades. Both glaciations are thought to have ended as a result of a buildup of high concentrations of greenhouse gases that eventually overwhelmed the ice albedo effect, and led to a rapid deglaciation, hothouse conditions, and worldwide deposition of cap carbonates (Hoffman et al., 1998; Hoffman and Schrag, 2002). The climatic and chemical peculiarities of this time are also deemed responsible for various

morphological oddities in cap carbonates (James et al., 2001; Hoffman and Schrag, 2002; Allen and Hoffman, 2005; Corsetti and Grotzinger, 2005; Hoffman and Macdonald, 2010; Lamb et al., 2012).

Cap dolostones deposited after the Sturtian glaciation on the Congo Craton in Namibia record a condensed transgressive systems tract (TST) and relatively deep water environments at the base, and a shallowing upwards in a thick highstand systems tract (HST) through most of the Cryogenian Rasthof Formation (Hoffman and Halverson, 2008; Pruss et al., 2010). Near the town of Sesfontein in northern Namibia, dark, micritic, and typically stratiform microbialaminites are prevalent in the Rasthof Formation, which sharply overlies Sturtian glacial strata. Some facies of the lower Rasthof Formation preserve cm-scale roll-up structures, which are made up of several layers of microbially laminated dolomite or dolomitic limestone that have folded back or rolled up on themselves. Facies patterns in the Rasthof Formation vary laterally as do carbon isotope profiles, which suggest asynchronous deposition on a complex post-glacial topography (Pruss et al., 2010), due in part to glacial erosion and in part to active normal faulting throughout deposition of the Rasthof Formation and into the overlying Gruis Formation (Hoffman and Halverson, 2008). Roll-up structures are laterally extensive in the Rasthof Formation and are present locally in Cryogenian cap carbonate sequences on the Kalahari craton of southern Namibia and on the North Slope subterrane of Arctic Alaska (Macdonald et al., 2009b; 2010), suggesting broadly contemporaneous deposition of this type of microbialite on multiple paleocontinents. However, the Cryogenian cap carbonates of the Kalahari craton, Arctic Alaska, Mongolia, and NW Canada formed in TSTs equivalent to only the lowermost portion of the Rasthof Formation (Macdonald et al., 2009a; Rooney et al., in review). This correlation, grounded in carbon and strontium isotope chemostratigraphy, demonstrates that the Rasthof negative carbonate carbon-isotope anomaly is also relatively condensed, perhaps due to active tectonism during deposition of the Rasthof Formation. The global presence of roll-up structures in both the post-glacial TST and the subsequent HST suggest that the conditions that facilitated microbialite formation persisted long after deglaciation.

Carbonate facies of the lower Rasthof Formation contain thickly (Fig. 1A) and thinly (Fig. 1B–D) laminated carbonates that carry unambiguous microbial signatures. The visible laminae of thinly laminated microbialites are 0.1–1 mm thick (Fig. 1C, D), and form 0.3–10 cm-wide folds, contorted beds, and roll-up structures (Pruss et al., 2010). Individual visible laminae contain finer, dark, organic-rich 10–100 μm thick laminae. These microscopic laminae, preserved in dolomite crystals smaller than 20 μm, are separated by 20–50 μm light laminae made by more coarsely crystalline dolomite (Pruss et al., 2010). Identical, thin, formerly cohesive, and organic-rich laminae are present in the thickly laminated microbialaminites of the lower Rasthof Formation, but there, individual layers of dark laminae are separated by mm-thick light laminae composed of 100–200 μm-wide, coarse dolomite crystals with abundant organic inclusions (Pruss et al., 2010). The laminae of the thickly laminated microbialaminites can form 10 cm- to 0.5 m-wide folds (Fig. 1A), but the thickly laminated facies lack roll-up structures. The thickly and thinly laminated microbialaminites often interfinger, and both contain abundant carbonate intraclastic cement-rich veins and dikes that cut the bedding at various angles (Pruss et al., 2010). The deformation of 3–10 cm-thick mats into roll-ups and 10–50 cm-tall folds without breaking required cohesive but mostly unlithified mats. Therefore, extensive cementation occurred multiple centimeters below the microbialite-water interface.

Mechanisms that locally deformed the thick, otherwise stratiform mats of the lower Rasthof Formation remain debated and may have varied laterally. Roll-up structures are relatively uncommon in the rock record, but typically are associated with peritidal, upper intertidal, or even terrestrial environments where microbial mats are fractured, folded, and contorted by desiccation, waves, currents, or fluid escape (e.g., Demicco and Hardie, 1994; Simonson and Carney, 1999; Schieber et al., 2007). There, roll-up structures occur together with polygonal cracks, mud and mat chips, storm deposits, tidal channels, ripples, and evaporitic minerals (Schieber et al., 2007). Evaporitic minerals, polygonal desiccation cracks, and other indicators of shallow environments are also present in modern and ancient carbonate-depositing lakes where thick stratiform microbialites are preserved by in-situ precipitation of carbonate minerals, but lack roll-up structures

FIGURE *1*.—Microbialites from the Cryogenian lower Rasthof Formation, Namibia. A) Thickly laminated, undulating microbialaminites with folds (arrows) and dikes (outlined by dashed lines); interiors of folds are cement-rich and not laminated, supporting an origin by deformation and not by preferential microbial growth on topographic highs, as would be expected for stromatolites. B) Thinly laminated, stratiform microbialaminites; white dashed lines outline areas with abundant roll-up structures. C) Close-up of a roll-up structure from area pictured in B) in otherwise stratiform thinly laminated microbialaminites. D) Same field of view as in C; dashed lines outline two individual laminae of the roll-up structure.

(e.g., Défarge et al., 1994; Tribovillard et al., 2000). In contrast to these shallow water deposits, dark microbialaminites from the lower Rasthof Formation in northern Namibia extend over hundreds of kilometers, but lack evidence for sediment grains, storm deposits, tidal channels, bedforms, mud and mat chips, desiccation cracks and desiccation polygons (Hoffman and Halverson, 2008; Pruss et al., 2010). Cross-stratification, columnar stromatolites and other indicators of shallow water environments are reported at a more proximal locality of the Rasthof Formation (Le Ber et al., 2013), and are also present in the upper Rasthof Formation in northern Namibia. Thus, some facies of the Rasthof Formation do record shallow water deposition, but the absence of shallow water indicators from much, or all, of the lower Rasthof Formation, implies a deeper depositional environment (Pruss et al., 2010). This inference can be tested further by asking how the morphology and disruption patterns in Rasthof microbialites match those reported in modern mats that grow in shallow environments.

Macroscopic mat morphology in the presence of flow

The smooth, stratiform, undisrupted areas of the Rasthof microbialites (Fig. 1B, C) depart from the expected morphology of mats that grow in the presence of flow. Observations and experiments show that flow imparts a characteristic mm- to cm-scale surface roughness on mats even when sediment grains are absent. Alkaline hot springs in Yellowstone National Park contain very shallow zones with stratiform photosynthetic mats (Brock, 1978), and small ponds with low surface-flow velocities where submerged cyanobacterial mats form regularly spaced cm-wide pinnacles or flat-topped structures (Walter et al., 1976; Brock,

1978; Petroff et al., 2010). In areas where velocities typically exceed 5 cm/s, ~0.5 cm-thick photosynthetic mats elongate in the direction of the flow, forming approximately 1 cm-wide ridges (Petroff et al., 2010; Bosak et al., 2013, fig. 3A, C). In turbulent environments, filamentous streamers oriented in the mean direction of the flow emerge (e.g., Besemer et al., 2007). Streamers are reported in photosynthetic mats as well as in various aphotic environments (Johnson and Hallberg, 2003; Niederberger et al., 2009), indicating that strong flow can change metabolically distinct mats into similar morphologies. Mm-scale laboratory experiments with biofilms grown in the presence of laminar flow with velocities below 1 cm/s also create 10–20 μm-wide ridges and streamers spaced by about 300 μm (Battin et al., 2003; Besemer et al., 2007). This spatial heterogeneity is attributed to the coupling of biofilm growth and hydrodynamics: biofilm growth locally reduces the flow section, increases flow velocity, and promotes biofilm detachment (Besemer et al., 2007; Radu et al., 2012).

Interactions between mat roughness, bedforms, and flow also dictate the dissipation of energy at the bottom of the bed, and create spatial patterns through mat erosion and detachment. These interactions typically are associated with turbulent regimes (Reynolds number, Re > 1000) with length scales larger than 1 dm and velocities larger than 1 cm/s (e.g., experiments by Graba et al., 2010). Mats growing on clasts can reduce the roughness of the bottom substrate (Godillot et al., 2001), but filamentous surfaces can increase the bed roughness (Nikora et al., 1997) and the turbulent kinetic energy in the system (Labiod et al., 2007), enhancing biofilm detachment. In addition, hydrodynamic conditions during microbial growth can influence mat strength and biomass detachment in turbulent systems (Graba et al., 2013). The coupling between mat roughness and shear stress also has been proposed to contribute to the formation of topographic highs in mats and stromatolites (Tice et al., 2011).

To the extent that comparable flow conditions produce similar macroscopic mat morphologies, mats from environments where the flow periodically mobilizes sediment or erodes mats should acquire macroscopic roughness, seen as topographic features at mm, cm, dm and m scales. This roughness is preserved by the same cementation processes that preserve the much finer microbial laminae. For example, mud chips and intraclasts preserved within the dark, finely laminated and occasionally rolled-up microbialites from the pre-Sturtian Beck Spring Dolomite exposed in Death Valley attest to microbial growth in the presence of currents and waves (Harwood and Sumner, 2011). Importantly, comparable features are absent from the thickly and thinly laminated microbialaminite facies in Cryogenian cap carbonates of the lower Rasthof Formation, although lithification preserved the very fine 10–100 μm dark laminae and 0.1–1 mm large eukaryotic microfossils (Pruss et al., 2010; Bosak et al., 2011).

Disruption patterns in cohesive mats

Deformation patterns of modern, thick, and cohesive mats can help determine whether mats from the lower Rasthof Formation were disrupted by episodic strong currents. Modern, smooth, 2–5 mm thick marine microbial mats that grow in the presence of very low flow (1.5 cm/s) and rare sediment grains (Neumann et al., 1970) offer plausible mechanical analogs for the cohesive properties of the Rasthof mats. These modern mats, which are made by filamentous cyanobacteria, grow in the troughs between 30 m-wide sand waves and contain fine organic laminae (Neumann et al., 1970) that resemble the lamination in the Rasthof microbialaminites (Pruss et al., 2010). Whereas the presence of sand waves suggests an energetic environment, the rarity of trapped and bound grains in the thick modern mats indicates that these mats grow during quiescent times when the sediment grains do not move. Indeed, the growth of microbial mats in any environment depends on the duration of quiescent times as well as the distribution and frequency of disruptive events that mobilize sediments (Mariotti and Fagherazzi, 2012). Observations from different environments and systems constrain the duration of these quiescent times to at least two weeks (Uehlinger et al., 1996; Labiod et al., 2007).

Shear stresses induced by flow create predictable disruption patterns in the cohesive, thick, natural mats (Neumann et al., 1970) and in laboratory systems (Labiod et al., 2007; Graba et al., 2013). The smooth, previously undisrupted areas rupture and break off as 2–3 cm wide and 0.5 mm thick flakes when the experimentally imposed horizontal currents above the mat exceed 50 cm/s (Neumann et al., 1970). The flakes are transported by the flow, leaving pits that are 0.5 mm deep and 2–3 cm wide in the mats (Neumann

et al., 1970). In gelatinous mats that contain fewer filamentous cyanobacteria and more unicellular, coccoidal, or sausage-shaped microbes and exopolymeric substances, the disruption occurs at lower current velocities (around 30 cm/s) and mats are eroded into 0.5–1 cm wide aggregates rather than peels (Neumann et al., 1970). The flow velocities required to disrupt undisturbed mats exceed the typical velocity of tidal currents in environments colonized by mats, and are comparable to the flow velocities in tidal channels where mats do not grow (Scoffin, 1970). Thus, the high flow velocities required to disrupt microbial mats in the lower Rasthof Formation would have created channels, bedforms, pits, and flakes. Again, none of these are present in the laterally extensive, thickly and thinly laminated Cryogenian microbialaminites.

A more plausible explanation for the localized disruption of the thick Rasthof microbialaminites and the presence of abundant, syndepositional dikes is disruption from below by expulsion of fluids in subtidal environments (Pruss et al., 2010). This deformation mechanism can account for the presence of abundant dikes and cracks, and for the three-dimensional fold-like morphology of individual roll-up structures (Fig. 1C, D). The deformation of mats and fluidization below storm wave base may have been aided by seismic events and synsedimentary faulting, which were active throughout deposition of the Rasthof Formation (Hoffman and Halverson, 2008). It is difficult to explain the folds by simple slumping because they lack a coherent vergence direction (Pruss et al., 2010).

Implications for carbonate deposition rates in post-Sturtian microbialaminites

The preservation of sub-wavebase microbialaminites in the Cryogenian Rasthof Formation underscores a higher preservation potential below the mat-water interface during this time. This was effected by the extensive precipitation of carbonate minerals around organic surfaces below the mat-water interface (Pruss et al., 2010). The preservation and deformation of these microbialites may have been facilitated by the same chemical factors responsible for the widespread cementation of the seafloor during the Archean and Proterozoic (Grotzinger and Knoll, 1999; Higgins and Schrag, 2003; Higgins et al., 2009; Bosak et al., 2013) and the preservation of roll up structures in Archean microbialites (Fig. 2), which also were interpreted as deep-water facies (Simonson and Carney, 1999; Schröder et al., 2009). Moreover, the fine, dark, 10–100 μm-thick laminae in the microbialites of the lower Rasthof Formation are comparable to fabrics in older Neoproterozoic microbial carbonates that predate the Sturtian glaciation (Turner et al., 2000; Mata et al., 2012), suggesting that carbonate depositional rates and taphonomic conditions in the lower Rasthof Formation were not that different from conditions before the Sturtian glaciation.

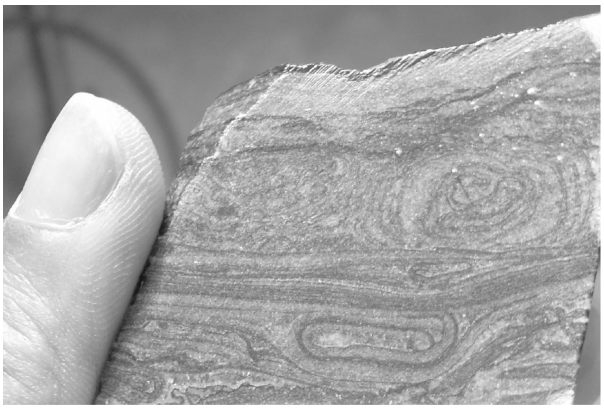

FIGURE 2.—Roll-up structures in Archean microbialaminites from the 2.6—2.5 Ga Campbellrand Platform, Transvaal Group, South Africa.

Laboratory experiments that explore the formation and preservation of microbial textures in carbonates can inform estimates of the carbonate deposition rates in the Rasthof Formation. These rates have not been constrained to date. Photosynthetic mats that grow in laboratory cultures in the presence of nearly mM concentrations of nitrate and phosphate and 10–100 mM concentrations of inorganic carbon (i.e., non-limiting nutrient concentrations), and optimal light and growth temperatures take about one month to grow to ~ 0.5–2 mm thick (Bosak et al., 2009, 2010). Evaluated both for microbes adapted to temperatures above 45 °C and those adapted to cooler environments, these rates are consistent with a recent report of fast, cm/yr stromatolite accretion rates in a hot spring (Berelson et al., 2011), and are likely to be the biological upper limit for the Rasthof mats. Microbial growth will be slower when conditions are suboptimal (Bosak et al., 2009), as was likely the case in deep, possibly light-limited or aphotic Cryogenian microbialaminites. These growth rates indicate that the mm-thick lamination of microbialaminites from the lower Rasthof Formation could be seasonal, but not diurnal. If microbial mats

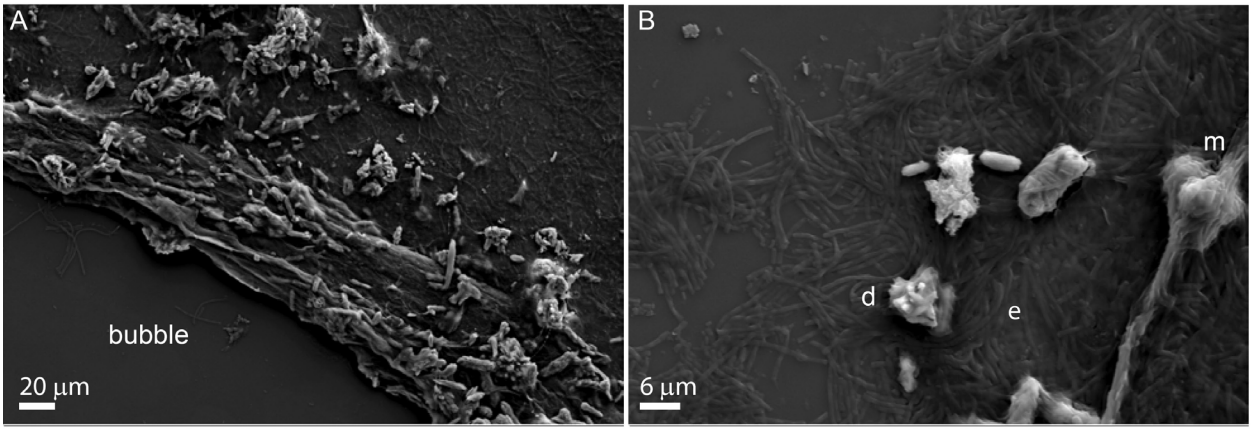

FIGURE *3*.—Scanning electron micrographs of 30 μm-thick sections showing lithification in a laboratory-grown cyanobacterial mat, where the initial culture medium was in equilibrium with 5% pCO_2 at pH 7.5, and contained little sulfate (composition of the lithifying medium, growth conditions, and the sample preparation are described in Bosak et al., 2010). The culture was incubated for two months before analysis. A) Picture showing precipitation of $CaCO_3$ around aligned cyanobacterial filaments. The mineral, seen in the light-colored areas and as small mineral grains, preserves a thin microbial lamina. The lower left area contained a gas bubble and remained mineral-free; the upper-right area contains randomly aligned filaments, small, sausage-shaped cyanobacteria, and exopolymeric substances; randomly distributed crystals of $CaCO_3$ that nucleated on the biomass in this region can be seen as light-colored particles and regions. B) Fine-grained calcium carbonate precipitated around a thin lamina that contains aligned filamentous cyanobacteria (light-colored continuous strand); m shows a larger crystal that nucleated off the lamina; *d* shows larger crystals of $CaCO_3$ that nucleated in the adjacent region; *e* marks an area filled with randomly aligned filamentous cyanobacteria embedded in exopolymeric substances. Total thickness of the precipitated mineral in the entire mat was ~100 μm.

maintained a plastic, cohesive, mm- to cm-thick layer above the more fully lithified layer (Fig. 1) instead of being smothered by carbonate minerals, the biological growth rates had to have outpaced carbonate sedimentation. The observed rates of mat growth under optimal conditions (0.5–2 mm/month, or 6–24 m/kyr) thus constrain carbonate sedimentation rates to less than 6 m/kyr. Experiments investigating the preservation of microbial textures and biosignatures in rapidly precipitating systems also require rates lower than 5 μm/day or 2 m/kyr: more rapidly precipitating minerals either smother microbial biofilms, or fail to preserve continuous, finely micritized, organic-rich laminae and microbial microporosity (Bosak et al., 2004) comparable to the textures of the Rasthof microbialaminites (Pruss et al., 2010).

The preservation of modern textural analogs of the Rasthof mats can also refine estimates of the lowest carbonate accumulation rates required to preserve comparable textures. In the laboratory, where T, pH, and DIC conditions favor carbonate precipitation, it takes about two months to deposit an approximately 20 μm-thick layer of micritic calcium carbonate around a fine microbial lamina and more irregular minerals in areas rich in exopolymeric substances (Fig. 3) (Bosak et al., 2010, 2012), producing 50–100 μm of minerals within the entire laminated mat. Therefore, lithification rates required to preserve the fine 10–100 μm laminae of the Rasthof mats would have been at least 120 μm/yr (12 cm/kyr), but lower than 2 m/kyr. These rates are not extraordinary, and are comparable to those found on modern shallow-water carbonate platforms (e.g., Milliman, 1993). Notably, intermittent, locally higher rates of carbonate precipitation within the thickly laminated microbialaminites may have outpaced the growth of microbial mats, forming the light-colored inclusion-poor 0.5–2 mm laminae that often contain early marine bladed cements (Pruss et al., 2010). This thickly laminated facies is ubiquitous through ~30 m of the Rasthof at Ongongo and Okaaru (Pruss et al., 2010), and may mark intervals and areas with faster carbonate accumulation rates relative to those in the overlying roll-up facies characterized by thin, microbial laminae.

MICROBIAL STRUCTURES IN BASAL EDIACARAN CAP CARBONATES

Basal Ediacaran cap carbonates predominantly formed in transgressive systems tracts without

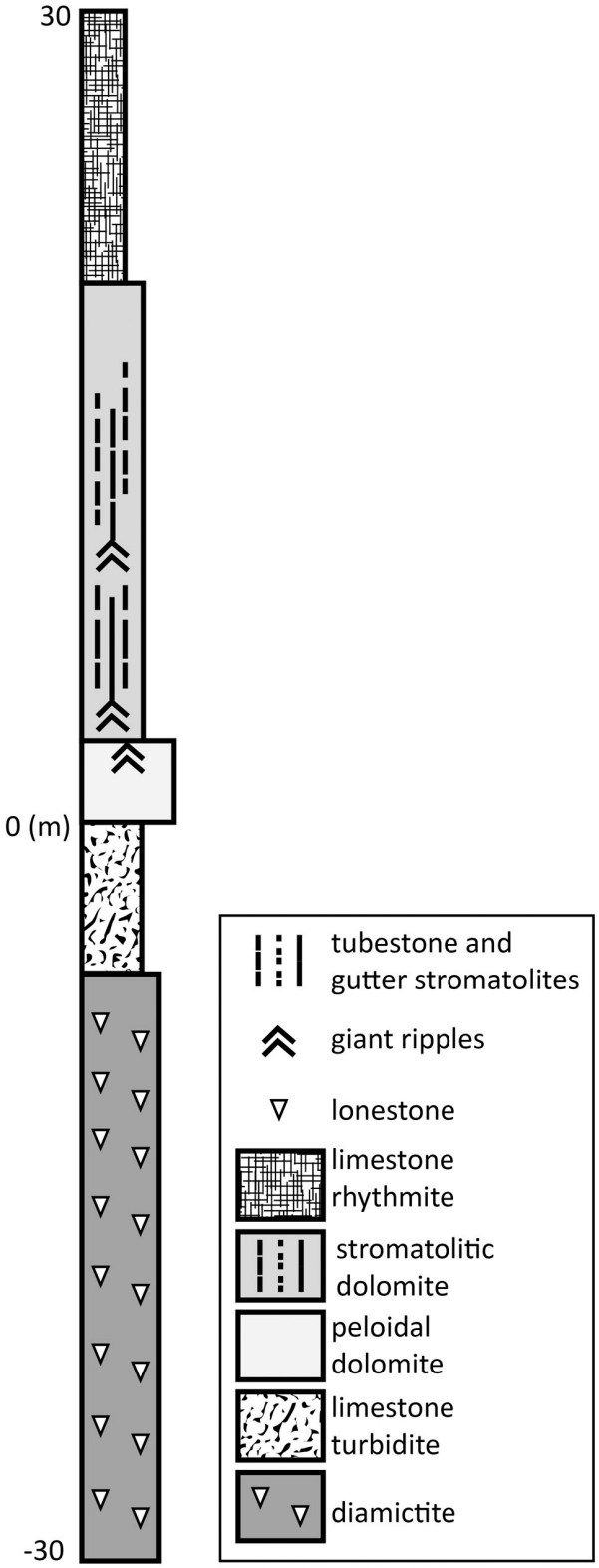

FIGURE *4*.—Generalized stratigraphic column of the Dreigratberg cap carbonate at Namaskluft Camp (modified after Hoffman and Macdonald, 2010).

obvious subsidiary parasequences. One exception to this trend is the Dreigratberg cap carbonate in southern Namibia and South Africa, where the progression from graded, thin-bedded limestones at the base to wave-rippled peloidal dolostone at the top has been attributed to a regression prior to the glacio-eustatic transgression, perhaps due to ice gravity effects (Hoffman and Macdonald, 2010), or to glacio-isostatic rebound. These interpretations are associated with different timescales of cap carbonate deposition: ice-gravity effects are expected on sub-kyr timescales, and isostatic rebound occurs on 10 kyr timescales.

The typical facies of basal Ediacaran cap dolostones are petrographically and stratigraphically distinct (Hoffman, 2011). They record a transgressive sequence and contain morphologically unique sedimentary structures, including giant ripples, and tube-hosting and corrugated stromatolites (Figs. 4–6) (Cloud et al., 1974; Hegenberger, 1987; Aitken, 1991; James et al., 2001; Hoffman and Schrag, 2002; Allen and Hoffman, 2005; Corsetti and Grotzinger, 2005; Jerolmack and Mohrig, 2005; Hoffman et al., 2007; Hoffman and Macdonald, 2010; Hoffman, 2011; Lamb et al., 2012). Both stromatolites and mechanically bedded facies in the cap dolostones exhibit prominent mm-scale lamination, and contain characteristic opaque and clotted textures and macropeloids (Kennedy, 1996; Calver and Walter, 2000; James et al., 2001; Fraiser and Corsetti, 2003; Halverson et al., 2004; Xiao et al., 2004; Corsetti and Grotzinger, 2005; Jiang et al., 2006; Hoffman et al., 2007; Giddings and Wallace, 2009; Hoffman, 2011). Tube-hosting and corrugated stromatolites, giant ripples, macropeloids, and the clotted textures typically are interpreted as records of uncommonly high carbonate deposition rates and rapid cementation during deglaciation (Fraiser and Corsetti, 2003; Corsetti and Grotzinger, 2005; Hoffman et al., 2007; Hoffman and Macdonald, 2010; Hoffman, 2011). These unusual sedimentary features are discussed below, and some experimentally testable hypotheses about microbial interactions with carbonate minerals and flow during the deposition of basal Ediacaran cap carbonates are proposed.

Textural evidence for microbial presence in giant ripples, corrugated stromatolites, and tubestone stromatolites

The prominently laminated facies of basal

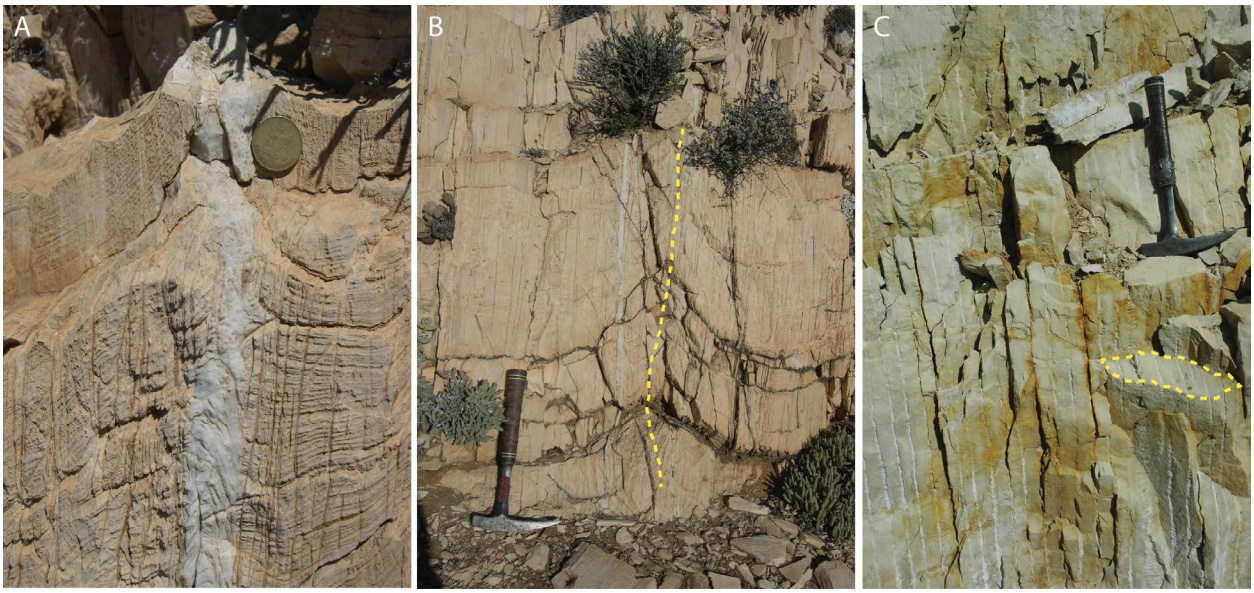

FIGURE *5*.—Elongated stromatolites in basal Ediacaran cap carbonates. A) Elongated, cm-wide stromatolite nucleated on the crest of a giant ripple from the Dreigratberg cap carbonate of the Gariep belt, Southern Namibia; Namibian coin is approximately the size of a US quarter. B) Elongated, cm-wide stromatolite (light grey) nucleated on the slope of a giant ripple from the Dreigratberg cap carbonate; yellow dashed line marks ripple crest; hammer for scale. C) Vertical and horizontal (dashed yellow line) cross-sections through gutter-like elongated stromatolites from the Ravenstroat cap carbonate in northwestern Canada; elongation is visible in the horizontal area outlined by the dashed line; hammer for scale.

Ediacaran cap dolostones can be either normally or inversely graded, and contain strong evidence of carbonate precipitation around organic nuclei and microbial surfaces. The best-preserved examples of these facies are characterized by pseudopeloidal (Corsetti and Grotzinger, 2005) or micropeloidal textures (James et al., 2001) composed of dark clots, 50–200 µm in diameter. The same clotted textures are present in mm-scale macropeloids that were easily fragmented, and are variably compacted (James et al., 2001; Corsetti and Grotzinger, 2005). The micropeloidal or pseudopeloidal clotted textures are more common in stromatolite facies, whereas macropeloids are more common in the mm-thick, inversely graded laminae of giant wave ripples and in other non-rippled but laminated facies (James et al., 2001). The interfingering laminae on the ripple crests and the sinusoidal vertical migration of the ripple crests demonstrate accretion by the delivery of light, organic-rich grains in the presence of oscillatory flow (Hoffman and Schrag, 2002). Interpretations of megaripples invoke subtidal conditions affected by extreme and repeated hurricanes (Allen and Hoffman, 2005), or much more normal wave conditions (Lamb et al., 2012). The latter model assumes that particles in ripples were mostly coarse and fully lithified to account for the trochoidal shape of megaripples and the roundedness of macropeloids, but does not explain the presence of finer, micropeloidal/pseudo-peloidal laminae in megaripples (e.g., figure 2 in Lamb et al., 2012; James et al., 2001). These features are identical to clotted textures produced in microbial mats and are unlikely to have originated by the recrystallization of macropeloidal laminae. The presence of these microscopic textures in the macroscopic bedforms is unusual. If ripples and stromatolites were generated by conditions that regularly moved coarse, dense sediment grains, why are intraclasts and composite grains notably absent from the rippled and stromatolitic facies of basal Ediacaran cap dolostones? Even more confusingly, if megaripples formed in areas where mats would be eroded by the transport of coarse and dense granular sediment, why are clotted, peloidal, and pseudopeloidal biologically influenced textures (Halverson et al., 2004) the principal component of these macroscopic structures? These questions invoke situations and scenarios that rarely occur in carbonate-depositing environments.

The striking abundance of clotted textures in megaripples and stromatolites offers insights into chemical and biological conditions that operated during the deposition of basal Ediacaran cap

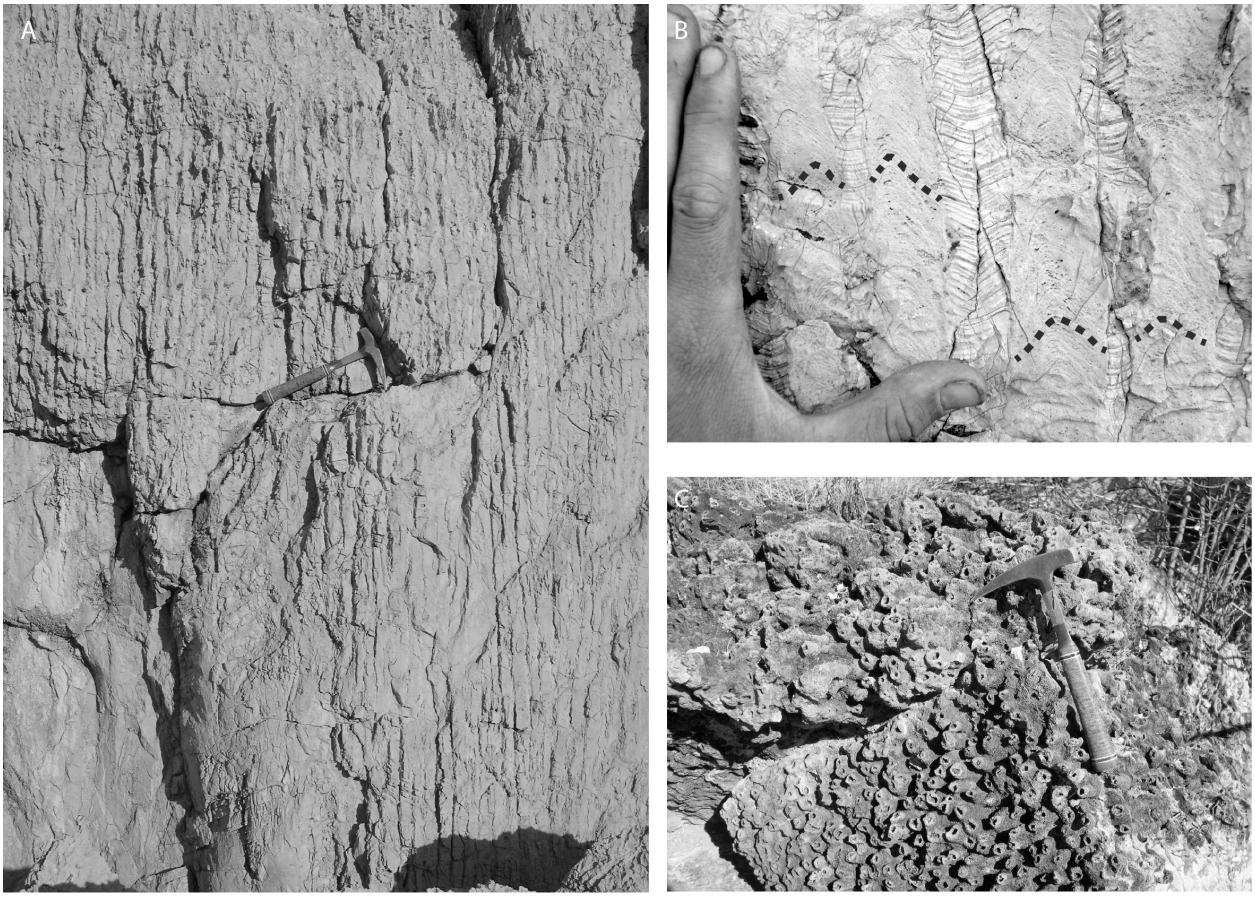

FIGURE *6*.—Tubes in stromatolites from a Marinoan cap carbonate, Otavi Platform, northern Namibia. A) Vertical cross-section; hammer for scale. B) Closer view of vertical cross-section; note the relatively low synoptic relief between the convex stromatolite laminae and the adjacent micritic fill in the concave tubes. C) Top and side view of silicified tubes; hammer for scale.

dolostones. As noted by previous studies (Wright et al., 1978; James et al., 2001; Corsetti and Grotzinger, 2005), the principal textural units in the laminated facies of basal Ediacaran cap dolostones—microbially-controlled clots—are not unique to this time interval. Clotted carbonates are present in modern and ancient microbialites (e.g., Monty, 1976; Reid, 1987; Sun and Wright, 1989; Buick and Dunlop, 1990; Gregg and Shelton, 1990; Sami and James, 1994; Kaźmierczak et al., 1996; Trichet et al., 2001; Dupraz and Visscher, 2005; Riding and Tomás, 2006; Spadafora et al., 2010; Perri et al., 2012). These features form by the precipitation of micritic carbonate in microbial mats and around suspended microbes (Trichet and Défarge, 1995; Kaźmierczak et al., 1996; Arp et al., 1999; Sprachta et al., 2001; Dupraz and Visscher, 2005; Spadafora et al., 2010), or by diagenesis of micritized microbial laminae (Turner et al., 2000). All of these mechanisms depend on the interactions between microbial metabolisms, organic surfaces, and the saturation state of the solution with respect to carbonate minerals (Arp et al., 1999; Bosak and Newman, 2005; Dupraz and Visscher, 2005). Although peloids can precipitate around inorganic nuclei in solutions that are not strongly saturated with respect to calcium carbonate (Bosak et al., 2004), the presence of dark inclusions throughout the clots, the lack of extensive cement-rich rims, the deformability and erodibility of facies with clotted textures, and the similarity of these textures to demonstrably microbial carbonates that form in surface-attached microbial mats (see references above), argue for a microbial origin of clotted textures in basal Ediacaran cap dolostones (James et al., 2001; Fraiser and Corsetti, 2003; Corsetti and Grotzinger, 2005). Moreover, the absence of extensive cement-rich rims, isopachous cements, and inclusion-poor dendritic crystals (Pentecost, 1990; Jones and Renaut,

1996; Chafetz and Guidry, 1999; Seong-Joo and Golubic, 2000) confines carbonate nucleation and precipitation primarily to organic matrices. Therefore, extensive mineral precipitation did not outpace microbial growth, as would be expected in environments that are highly saturated with respect to carbonate minerals (Pentecost, 1990; Jones and Renaut, 1996; Arp et al., 1999; Bosak et al., 2004; Bosak and Newman, 2005; Jones and Renaut, 2008; Okumura et al., 2012).

Clotted microbial carbonates occur among the abundant eukaryotically derived skeletal and bioclastic grains in various Phanerozoic carbonate sediments (Martín et al., 1997), and were common in microbialites that dominated skeleton-poor Phanerozoic reefs (Adachi et al., 2004; Baud et al., 2005) even during episodes of possible acidification (Payne et al., 2010). Therefore, the preponderance of clotted textures in the thick, rippled and stromatolitic facies of basal Ediacaran cap dolostones can be interpreted to indicate that: 1) carbonate deposition was strongly controlled by microbial processes; 2) the rate of carbonate deposition in shallow-water environments did not outpace the rate of microbial growth; 3) other carbonate depositing mechanisms played, at best, a minor role during the deposition of the stromatolitic facies; and 4) the saturation state of seawater with respect to calcium carbonate during the deposition of basal Ediacaran cap dolostones was comparable to the saturation state at other times in Earth history, including some proposed episodes of ocean acidification. In summary, the typical textures in mechanically graded and stromatolitic facies of basal Ediacaran cap dolostones offer little evidence for extraordinarily high mineral precipitation rates and seawater saturation states.

Hypothesis: 'Corn puffs in milk' model

If carbonate particles form almost exclusively around organic material, carbonate deposition rates have to trail bulk organic growth, and unlithified or partially lithified organic surfaces can be expected both on the seafloor and suspended in the water column. Erosion and suspension of clotted, sticky, and only partially lithified mats may have contributed to the unusual abundance of clotted macropeloids in basal Ediacaran cap dolostones. These grains are interpreted as aggregates of smaller, rolling, sticky, cohesive, organic-rich particles that eventually became lithified (James et al., 2001; Halverson et al., 2004; Hoffman, 2011). Laboratory experiments show that it is easy to form rounded, light, easily suspended microbial aggregates that can lead to macropeloids. Randomly shaped, 0.2 mm-wide suspended thin fragments of broken-up and lightly lithified microbial mats aggregate into mm-sized, rounded particles within a week (Fig. 7). If organic-rich particles remain sticky and suspended when microbial mats and clotted layers are ripped up or eroded, and the eroded material is only lightly lithified, irregular, rimless fragments of eroded mats may be difficult to recognize against an identical background of organic-rich, lightly lithified sediments. The "corn-puffs-in-milk" hypothesis does not require that mat pieces float on the surface of the liquid and remain suspended in the presence of very low flow, as would dry corn-puffs cereal. Instead, the rounded, light, organic-rich particles can be suspended by flow regimes that cannot suspend mm-sized carbonate grains.

The proposed model for the origin of macropeloids rests on the following assumptions: 1) most carbonate sediment incorporated into macropeloids originates as suspended, mm-sized,

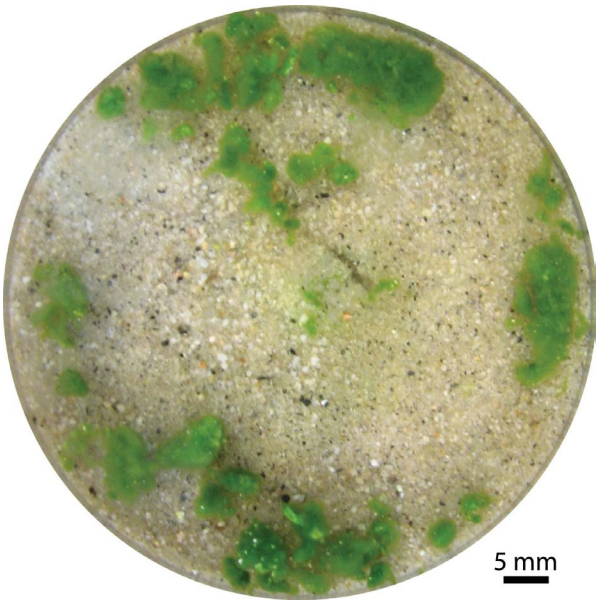

FIGURE 7.—Photo showing mm- to cm-scale rounded and sheetlike cyanobacterial aggregates formed in gently agitated artificial seawater. The culture container was inoculated using cyanobacterial mats dispensed through a needle-tipped syringe to form irregular fragments <0.5 mm wide. Gentle agitation by a rotatory shaker moved cyanobacterial fragments and aggregates, but did not move smaller quartz grains at the bottom.

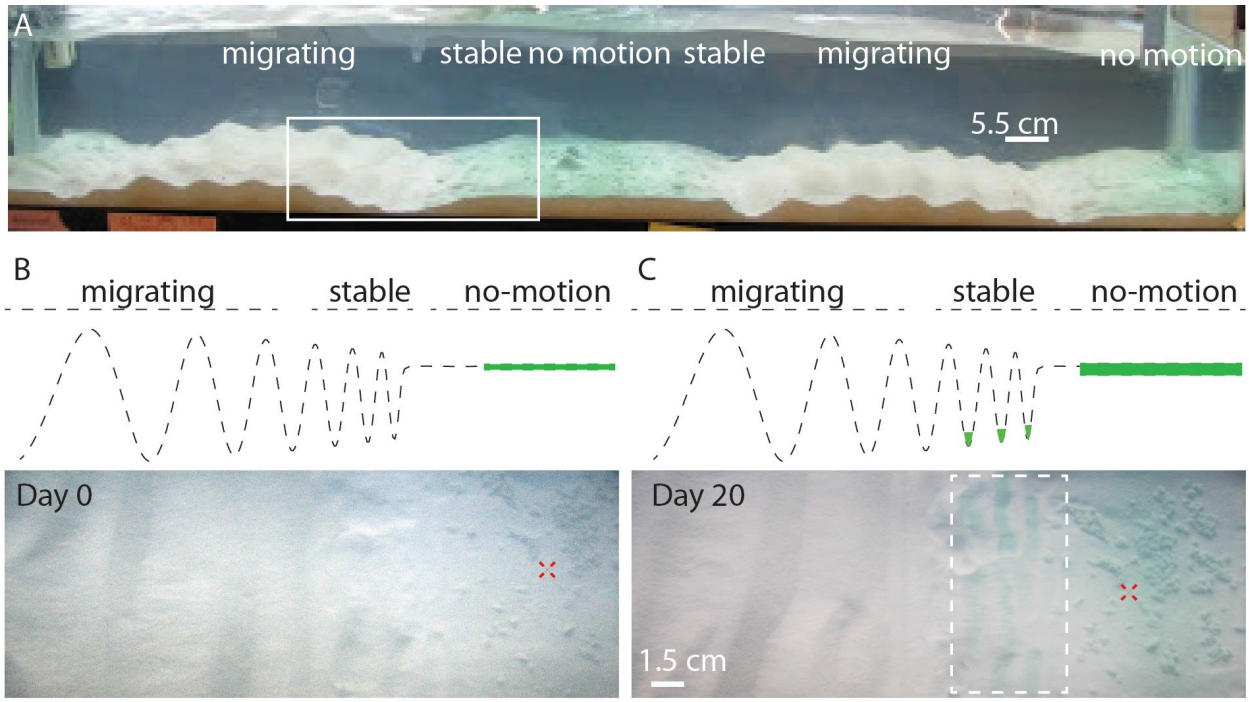

FIGURE *8*.—Cyanobacterial mat growing on aragonite sand in a tank forced with a standing wave. A) Photograph of side view of the tank. The amplitude of the surface wave and the bed shear stress are greater in areas where migrating ripples form and smaller on the sides and in the middle, where a flat bed is maintianed. Stable ripples form in areas with intermediate shear stress. Side view of the area shown in B and C is outlined by the white rectangle. B) Top view of the sterile tank just after the addition of fragments of tufted mats (Day 0). C) The same area as in B after 20 days of agitation. The mat grew on the flat bed and in the troughs of the stable ripples (dashed rectangle). Red crosses indicate the same location in B and C, respectively. The solution above the mat remained oxic throughout the experiment, and none of the topographic highs were cemented.

lightly lithified, sticky, organic-rich grains, or within microbial mats; 2) extensive lithification occurs only below the erodible mat-water interface; and 3) mechanically bedded sediments may have accreted in the presence of low flow regimes. These assumptions are consistent with the preponderance of clotted textures in basal Ediacaran dolostones, reports of truncated, fragmented, fused, and variably compacted larger peloids (James et al., 2001; Halverson et al., 2004), the absence of rip-up clasts, and the development of clotted mat textures in megaripples. If bedforms are present and composed of dense grains, mats grow preferentially in the troughs and on the lee sides of ripples (Fig. 8) (Gebelein, 1969; Schieber et al., 2007, fig 2.1.8A and figures 4C–12D), but not on the crests. Instead, if the suspended macropeloids were light (i.e., less dense), they may have been transported in low flow regimes that cannot suspend denser sediment grains, as is the case in the gently agitated laboratory cultures (Fig. 7). Consequently, megaripples could have accreted in flow regimes characterized by extended periods that permitted the growth of mats (at least months, Uehlinger et al., 1996; Labiod et al., 2007). This may explain the presence of microbially bound sediments in rippled areas where the transport of denser, mineral-rich sediment grains would have eroded microbial mats (Fig. 8) (Halverson et al., 2004; Hoffman and Macdonald, 2010), and the textural similarity between stromatolites and mechanically bedded facies in basal Ediacaran cap dolostones.

The proposed ‘corn-puffs-in-milk’ model of subtidal areas teeming with organic, easily transportable, partially lithified particles can be constrained by experiments that explore the formation and transport of rounded, microbial particles of relatively low density in the presence of weak and strong flow, respectively, and the response of microbially stabilized surfaces and topographies to the traction load of rounded mat fragments. These studies should also seek to determine lithification rates within microbial mats and organic-rich rounded grains under various

chemical, biological, and physical conditions to address the preservation and compaction of peloidal textures. Features and texture patterns generated in the laboratory also should be compared to the patterns of textures in the crests and troughs of the megaripples. Future modeling efforts should ask whether trochoidal ripples with large wavelengths can be generated in low flow regimes and by low-density, organic-rich, sticky particles.

Interactions between microbes, carbonate minerals, and flow in the laminated facies of basal Ediacaran cap dolostones

There is nothing particularly odd about the sub mm- and mm-scale textures in the visibly laminated, rippled, and stromatolitic facies of basal Ediacaran cap dolostones, yet these textures aggregate into unusual macroscopic forms that often are inherited over meters or tens of meters of stratigraphy (Fig. 4). In addition to megaripples (Fig. 5A, B), these forms include widely spaced, elongated stromatolites, corrugated stromatolites (Fig. 5C), and stromatolites surrounding tubular boundstone (Fig. 6). The following sections discuss these facies and implications for carbonate deposition rates in the aftermath of the Marinoan glaciation.

Widely spaced elongated stromatolites in basal Ediacaran cap carbonates.—Elongated stromatolites in basal Ediacaran cap carbonates are present in the Mackenzie Mountains of northwestern Canada (James et al., 2001; Hoffman and Halverson, 2011), the Congo craton of Namibia (Hoffman, 2011), and on the Kalahari Craton in the Gariep belt of Nambia and South Africa (Hoffman and Macdonald, 2010). The Dreigratberg cap carbonate of the Kalahari Craton at the Namaskluft Camp locality formed in a channel approximately 8 km across (Hoffman and Macdonald, 2010), and hosted elongated stromatolites interbedded with giant wave ripples (Hoffman and Macdonald, 2010; Macdonald et al., 2010; Fig. 5A, B). The stromatolites appear to have nucleated on or close to the crests of giant wave ripples, and their crests have the same 1–3 m spacing as the crests of giant ripples (Fig. 5A). The nucleation of stromatolites on ripple crests may be a consequence of more rapid cementation in the crests relative to all other areas (Fig. 5A). The resulting stromatolites are ~1 cm to 1 m wide, several m long, and become more abundant and closely spaced up-section through ~20 m of stratigraphy. Elongated stromatolites that nucleated on the crests of giant ripples at Namaskluft Camp appear to have modified flow conditions, changing the height and wave form of the ripples along strike between individual elongated stromatolites. If, as the textures would imply, the biological and flow conditions supported the growth of mats and the delivery of macropeloids everywhere, what processes may account for preferential cementation on ripple crests?

Hypothesis: Porewater pumping and the cementation of crests in giant ripples.—The initial cementation of the crests of giant ripples in basal Ediacaran cap carbonates requires an explanation that spatially couples cementation to the topography of giant ripples. This spatial pattern is consistent with the predicted patterns of porewater flow inside bedforms (Huettel and Gust, 1992; Huettel et al., 1998; Precht et al., 2004; Franke et al., 2006), where waves and currents pump solutes through porous sediments. The waves focus the flow from deeper layers into ripple crests, and currents focus the flow on the lee side of ripple crests (Fig. 9; Santos et al., 2012). The flow over and within unlithified megaripples could have induced preferential cementation close to or in ripple crests if more alkaline porewaters were transported from a deeper anoxic layer (Precht et al., 2004). Higher alkalinity within the sediments would be expected if they became anoxic close to the sediment and mat surface (Higgins et al., 2009) (Fig. 9C). Stabilized in this manner, the cemented hardgrounds in ripple crests would have maintained their position even in the presence of moving grains (Fig. 9D).

Implicit in the porewater-pumping mechanism are two hydrodynamic regimes: a more energetic flow, capable of moving macropeloids and creating the bedforms (Fig. 9B), and a less energetic flow that induces porewater flow, allows mat growth, and does not erode mats (Fig. 9C) (see experiments of Franke et al., 2006; Precht and Huettel, 2003). This scenario is consistent with observed variability in natural environments, where occasional storms are separated by long periods of sea breeze and regular tidal currents. Within this framework, the recurring higher energy conditions dictated the m-scale rippled topography and delivered macropeloids, whereas microbial mats colonized the bedforms during a less energetic regime that also allowed cementation and the inheritance of stromatolite topography. The morphology of giant

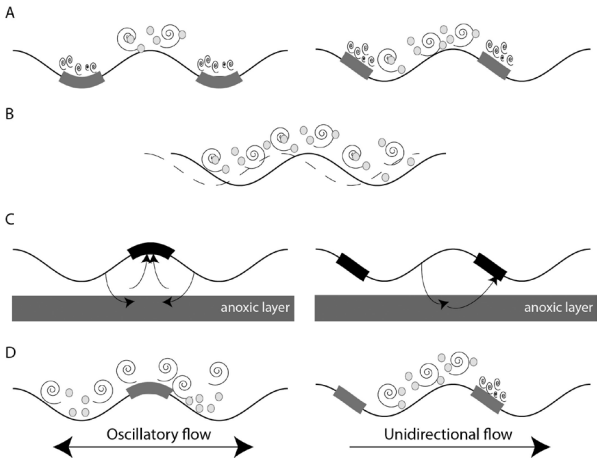

FIGURE 9.—Hypothesized interactions between mats and sand ripples; diagrams in A, C, and D show expected patterns created by oscillatory (l) and unidirectional (r) flow. Mats = thick grey areas; sediment = grey circles. A) Mats grow in areas with low shear stress (indicated by squiggly lines) and low sediment mobility. B) Energetic conditions that form migrating ripples destroy mats and prevent the formation of biofilm spatial patterns. C) Interactions between ripples and flow during less energetic conditions leads to porewater pumping. This process can promote cementation (thick black areas) in ripple crests and on lee sides of ripples by delivering anoxic, alkaline fluids from deeper layers. D) The newly formed hardgrounds facilitate microbial colonization, and are less easily eroded during subsequent high energy episodes.

wave ripples records symmetric oscillatory flow (Lamb et al., 2012), which would have produced porewater flow and may have induced cementation within the ripple crests. Porewater flow in other settings or during slack conditions also may have been driven by asymmetric surface flows, such as those associated with ebb- or flood-dominated tidal currents. Asymmetric flow typically would have occurred during the initial and final stages of development, when the crestlines of megaripples climbed obliquely (Allen and Hoffman, 2005). If so, the porewater flow during these times would have favored upwelling and cementation on the lee side of the bedform, not on the crest (Fig. 9C) (Santos et al., 2012), shifting stromatolites with respect to the ripple crest (Fig. 5B).

Further field observations, experiments, and calculations in systems similar to the one shown in Figures 7 and 8, can help evaluate the importance of porewater pumping, redox conditions in sediments, microbial colonization, and changing flow conditions for the formation of elongated stromatolites on preexisting topography. Detailed field observations at cm- and larger scales can help to identify petrographic and microchemical redox and textural gradients between the cemented and uncemented areas in ripple crests in various basal Ediacaran cap carbonates. A better understanding of ripple-associated basal Ediacaran stromatolites also may arise from experiments that test how microbes colonize rippled areas and hard grounds in the presence of moving, light, organic-rich particles. This colonization can be explored as a function of bedform geometry, porewater chemistry, and flow. Specifically, the porewater-pumping mechanism could be tested by experiments that compare patterns of cementation and biofilm growth as a function of porewater redox profiles from oxic to iron(II)-rich and sulfidic. Models of bed evolution can be adapted to account for differential cementation to quantitively test the proposed interactions between the cemented ripple crests and sand transport. Calculations of net porewater fields can also explore the robustness of the porewater-pumping mechanism as a function of the ratio of wave orbital diameter to formational orbital diameter, or the degree of asymmetry in the flow.

Narrowly spaced, corrugated stromatolites in basal Ediacaran cap carbonates.—At Namaskluft Camp, upsection from the facies containing giant ripples and elongated stromatolites spaced 1–3 m apart (Fig. 4), the Dreigratberg cap dolostone hosts narrowly spaced, elongated stromatolites (Hoffman and Macdonald, 2010; Macdonald et al., 2010) that are ~10 cm wide and separated by 0.5–2 cm-wide gutters that contain peloidal infill or are ribbed without fill. The inheritance of shape of stromatolites in these facies suggests that persistent erosion prevented coarsening upward or branching (Bosak et al., 2013). The corrugated surfaces of elongated stromatolites amalgamate into a 100 m-wide reef, which contains massive bioherms with tube-hosting stromatolites at the top. A similar pattern is seen in the Mackenzie Mountains of northwestern Canada, where elongated stromatolites are adjacent to giant wave ripples (Hoffman and Halverson, 2011). The narrowly spaced elongated stromatolites in the Mackenzie Mountains are similar to those in southern Namibia, and are separated by 0.5–2 cm-wide gutters that contain peloidal packstone. Vertical cross-sections through the narrowly

spaced elongated stromatolites and the overlying tube-hosting stromatolites, respectively, reveal similar, 0.5–2 cm-wide gaps (Figs. 5C, 6A). The presence of peloidal grains in these gaps suggests that the mat-covered areas in tube-hosting and corrugated stromatolites interacted similarly with the flow and sediments, but the topographic lows and peloidal sediment occupied less surface area and volume in tube-hosting facies.

Mounds of columnar stromatolites that form tube boundstone (Fig. 6) characterize many basal Ediacaran cap carbonate successions (Hoffman, 2011). Cloud et al. (1974) provided the most detailed description of the tubestone facies on a macro scale, reporting pinching and swelling of individual tubes with 0.5–2 cm diameters in large Noonday Dolomite stromatolite bioherms. Some tubes have a nearly circular cross-section (Fig. 6C), many are elliptical, some coalesce, and some are bridged by ~0.2–1 mm-thick clotted laminae (Corsetti and Grotzinger, 2005). Tube-hosting facies have been interpreted as: 1) vents by which methane escaped through microbialites from underlying permafrost (Kennedy et al., 2001); 2) stromatolites that formed in an environment greatly oversaturated with carbonate (Hoffman and Schrag, 2002; Corsetti and Grotzinger, 2005); 3) stromatolites shaped by a turbulent environment (Hoffman and Schrag, 2002); or 4) gas-release structures produced by organic decay within stromatolites (Cloud et al., 1974; Hegenberger, 1987; Hoffman et al., 1998). All four models assume fast precipitation rates of carbonate minerals, but invoke different biological processes, flow regimes, and general post-glacial environmental conditions (Hoffman et al., 2007). Because tubes typically are subvertical, Cloud et al. (1974) concluded that they formed through fluid escape, but did not specify the composition of the fluid. To account for the negative carbon-isotope signatures of cap carbonates and provide a source of alkalinity for carbonate precipitation, Kennedy et al. (2001) interpreted tubes as structures that released methane from underlying glacial sediments, although cements extremely depleted in ^{13}C, comparable to those from carbonates that accrete around methane seeps (Campbell, 2006), were not reported in any of the analyzed tubes. Carbonates that are very depleted in ^{13}C were reported in China (Jiang et al., 2003), but these are late-stage void-filling cements with a hydrothermal origin (Jiang et al., 2006; Bristow et al., 2011) and are not associated with stromatolitic facies. Methane release has been further criticized on the following grounds: the tubes rest on basement at some localities and do not tap into any underlying subglacial layers; methane could not provide enough alkalinity or carbon to explain the thickness or isotopic signatures of cap dolostones; and many of the tubes were filled with micrite in a concave-up meniscus that interfingers with the margins of the stromatolite on a micro-scale. This latter observation, along with the suggestion that tubestone bioherms formed predominantly on storm-dominated ramps in northern Namibia, led Hoffman and Schrag (2002) to suggest that the tubes aggraded as repeating pits in turbulent environments. Most recently, Corsetti and Grotzinger (2005) interpreted the tubestone facies as unusual stromatolite morphologies that formed independent of fluid escape. In this model, the convex stromatolite laminae grow mainly by in-situ precipitation of microclotted dolomite, whereas the tubes are filled by similar micrite or by late-stage sparry cement (Corsetti and Grotzinger, 2005). This model does not address or explain the precise inheritance of shape over meters of stratigraphy, and the subvertical orientation of tubes with respect to the paleohorizon (Cloud et al., 1974).

Hypothesis: Influence of inheritance, sedimentation, and gas production in the growth of tubestone stromatolites.—Morphological and sedimentological similarities between the corrugated stromatolites and tube-hosting facies (Figs. 5C, 6A) and the transition of the former to the latter (Fig. 4) imply that similar hydrodynamic mechanisms shaped both kinds of structures. The inheritance of topography over meters of stratigraphy requires a stabilization mechanism that prevented microbial growth in the gutters and tubes (Bosak et al., 2013). Differing amounts of peloidal infill in the gutters and tubes, respectively, indicate that fewer particles per unit horizontal area were delivered to the depressions of tubestone stromatolites, and more were eroding the gutters of elongated stromatolites. Preliminary laboratory observations confirm that erosion in these areas could occur if less dense, organic-rich particles moved in the topographic lows and also trapped some carbonate grains. The same mechanism may be responsible for the subvertical orientation of tubes: gravity delivers the mat-eroding particles to local depressions, and the flow moves these particles within depressions, thus eroding the mats. Both the erosion-control mechanism and the sediment load contributed to

the morphological differences between tubestones and gutter-like stromatolites. Because these mechanisms would have operated during deposition of most older and younger stromatolites, where tube-hosting stromatolites are absent, additional mechanisms are needed to explain the initiation and inheritance in tube-hosting stromatolites. A potential analog for the initiation of basal Ediacaran cap tubestones may be cyanobacterial mats that grow in dm- to m-deep waters of modern hot springs and develop numerous, cm-scale, O_2-rich blisters (Fig. 10) (Bosak et al., 2010). These mats contain spatial patterns similar to those in tube-hosting stromatolites, but are imperfect analogs in which to study the inheritance of pattern because they lack sediment grains and grow in a very low flow regime.

In the absence of modern or ancient analogs, laboratory experiments offer best hope of understanding the initiation and inheritance of patterns in tubestone stromatolites. To understand the inclination of tubes relative to the inclination of the surrounding stromatolite laminae, experiments should investigate the formation, propagation, and inclination of cm-scale topographic lows on even larger inclined surfaces, and the potential role of light, organic-rich particles in the maintenance of the topographic lows. The shared characteristics of elongated and tubestone stromatolites in basal Ediacaran cap carbonates also require that several different flow regimes be considered: 1) a higher energy flow regime that erodes mats and delivers sediment grains to topographic lows; 2) a lower energy flow regime that moves the eroded pieces around topographic lows, preventing microbial growth and lithification and maintaining the synoptic relief; and 3) an even lower energy flow regime that allows development of bridging laminae. Experimental systems can explore the interplay between these regimes (Fig. 8) with a focus on transitions between elongated and rounded patterns, the inheritance of topography in low flow regimes, and the presence of suspended organic debris.

Estimates of growth rates of stromatolites in basal Ediacaran cap dolostones.—Clotted-textured basal Ediacaran cap dolostones lack the fine, continuous laminae similar to those found in the Cryogenian microbialaminites of the lower Rasthof Formation. This may indicate lithification around non-filamentous organisms (Golubic, 1982; Browne et al., 2000; Arp et al., 2003),

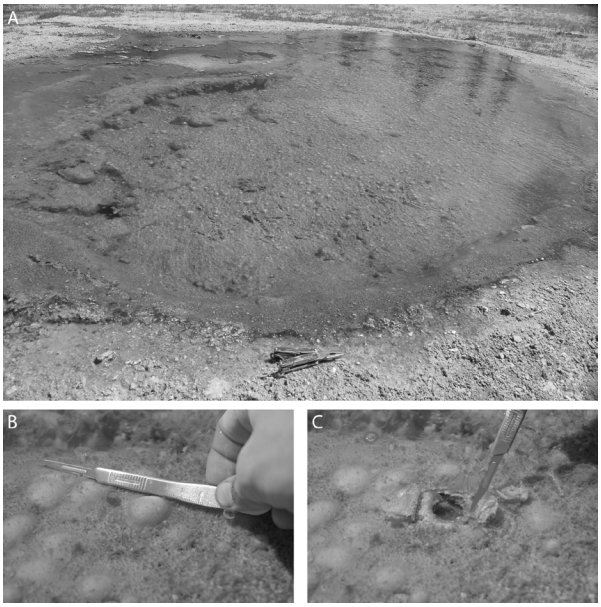

FIGURE *10*.—Centimeter-wide blisters within a photosynthetic mat in a hot spring in Yellowstone National Park, USA. A) An ~0.5 m deep hot spring pond; bright spots in the mat at the bottom are blisters. B) Close-up of blisters and adjacent mats. C) Same field of view as in B with central bubble broken, revealing a hollow, depressed interior.

random mineral precipitation within the exopolymeric matrix (Défarge et al., 1994; Arp et al., 1998, 1999; Dupraz and Visscher, 2005; Spadafora et al., 2010; Perri et al., 2012), more extensive degradation of the primary mat textures before mineralization relative to the conditions that preserved fine, continuous microbial laminae(Bontognali et al., 2010), and the recrystallization of fine laminae (Turner et al., 2000). Whatever the cause of lack of fine laminae, corrugated and tube-hosting stromatolites record a strong microbial influence on carbonate precipitation (James et al., 2001; Corsetti and Grotzinger, 2005), and allow estimates of carbonate deposition rates. If constraints on mat growth and lithification discussed in the earlier section about the Rasthof microbialites are applied to the stromatolitic facies in basal Ediacaran cap dolostones, they suggest carbonate deposition rates of not more than 2 m/kyr. This estimate is consistent with the growth of 10 cm-thick peloidal stromatolites in 2000 years or less (Perri et al., 2012), and rates of carbonate accumulation of 50 μm/yr or 0.5 m/kyr. These estimates can be improved by further studies of lithification rates and preservation of peloidal textures in modern environments and laboratory

systems.

These estimates of carbonate accumulation rates, derived from petrographic studies and temporal constraints on mat growth and lithification, require 20 kyr to deposit the 40 m-thick stromatolitic facies in some sections of the Dreigratberg cap dolostones (Hoffman and Macdonald, 2010), and even longer times to deposit the entire ~50 m-thick cap. Assuming that the unchanging stromatolite forms require persistent biological, chemical, and physical conditions, the thickness of stromatolitic facies in some cap dolostones (e.g., Fig. 4) also shows the remarkable persistence or recurrence of similar environmental conditions over tens of thousands of years. Overall, these estimates of carbonate accumulation rates in common facies of basal Ediacaran dolostones are: 1) comparable to accumulation rates in modern carbonate reefs (Milliman, 1993); 2) at least one to two orders of magnitude lower than the rate estimates that attributed the mm-thick peloidal laminae to diurnal forcing (Hoffman et al., 1998); 3) comparable to the lower estimates of average cap dolostone deposition rates which assume deposition during glacioeustatic rise (Hoffman et al., 2007); 4) higher than estimates of accumulation rates rooted in stratigraphic interpretations or paleomagnetic data (2–20 mm/kyr; Trindade et al., 2003; Kilner et al., 2005; Hoffman et al., 2007; Schmidt et al., 2009; Kennedy and Christie-Blick, 2011).

Neither the biological limit of how fast microbial mats can grow and lithify nor the petrographic evidence for strong microbial control of carbonate deposition supports extraordinarily fast or slow accumulation rates of Neoproterozoic cap dolostones. Given that carbonate deposition rates depend on the local saturation state with respect to carbonate minerals (Morse et al., 2007), and that the estimated carbonate deposition rates for the Rasthof microbialaminites and the peloidal stromatolites in basal Ediacaran cap dolostones are similar to the accumulation rates on modern shallow carbonate platforms, they imply comparable saturation states of post-Sturtian, post-Marinoan, and modern oceans. However, if Neoproterozoic cap carbonates only precipitated in subtidal areas, but not in the pelagic realm, the global saturation state in the post-glacial oceans may have been lower than that of the modern ocean, in keeping with the proposed equilibrium of high concentrations of atmospheric CO_2 at the time (Bao et al., 2008) and acidification (Kasemann et al., 2005, 2010). Laboratory experiments, studies of microbial carbonates, and microbial sedimentology offer tools with which to further explore this ancient world, rife with sedimentological oddities.

SUMMARY

Throughout geologic history, marine stromatolites have accreted in the presence of moving fluids, sediment grains, sticky microbial communities, and solutions that were variably saturated with respect to carbonate minerals. Changes in any of these physical, biological, and chemical processes can affect stromatolite shapes, sizes, and textures along environmental gradients and through time. Current attempts to use stromatolite shapes in environmental reconstructions produce non-unique answers about the influence of waves, currents, and the direction of paleoshorelines even in the case of the most typical forms, such as elongated stromatolites. Even more puzzling are rare or singular stromatolite forms: the roll-up structures in dark microbialaminites in the lower parts of the Cryogenian Rasthof Formation, and tube-hosting or elongated stromatolites associated with giant ripples that occur in a number of basal Ediacaran cap dolostones. Laboratory studies offer insights into conditions that shaped these forms. Widespread macropeloids and other confusing textural characteristics in the giant-ripple facies of basal Ediacaran cap dolostones led to the ‘corn puffs in milk’ model. This model invokes aggregation of microbial mat fragments into rounded, suspended particles and the transport of these large but light particles in flow regimes that permit microbial stabilization of sediments. Promising future directions for laboratory experiments and studies of microbial carbonates include studies of bedform formation in the presence of low-density organic particles and in low flow regimes, and experiments that explore lithification in microbial sediments as a function of surface flow and porewater chemistry. Of immediate utility are studies that explore timescales and conditions that enable the preservation of microbial textures in carbonates, particularly in the presence of low sulfate. These studies, when applied to the microbially-influenced textures found in the Cryogenian Rasthof Formation and various basal Ediacaran cap dolostones, estimate carbonate accumulation rates in cap carbonates comparable to those in modern reefs, but not substantially lower or

higher.

ACKNOWLEDGEMENTS

N. James and members of the Bosak lab helped with laboratory experiments. T. Bosak and F. Macdonald were supported by grants from NASA Exobiology and NASA Astrobiology Institute. T. Bosak and S. Pruss were also supported by the NSF Sedimentary Geology and Paleobiology Program (EAR-0843358). G. Mariotti was supported by the W. O. Crosby Postdoctoral Fellowship from EAPS, MIT. J. T. Perron was supported by the NSF Geomorphology and Land-Use Dynamics program under award EAR-1225865. Research permit #YELL-2008-SCI-5758 from the U.S. National Park Service enabled visits to sites in Yellowstone National Park. P. Hoffman's thoughtful comments inspired much of the discussion about timescales and macropeloids. Comments by F. Corsetti and A. Bush also improved the manuscript.

REFERENCES

ADACHI, N., Y. EZAKI, AND J. LIU. 2004. The fabrics and origins of peloids immediately after the end-Permian extinction, Guizhou Province, South China. Sedimentary Geology, 164:161–178.

AITKEN, J. D. 1991. The Ice Brook Formation and post-Rapitan, Late Proterozoic glaciation, Mackenzie Mountains, Northwest Territories. Geological Survey of Canada Bulletin, 404:1–43.

ALLEN, P. A., AND P. F. HOFFMAN. 2005. Extreme winds and waves in the aftermath of a Neoproterozoic glaciation. Nature, 433:123–127.

ALTERMANN, W. 2008. Accretion, trapping and binding of sediment in Archean stromatolites—morphological expression of the antiquity of life. Space Science Reviews, 135:55–79.

ARP, G., J. HOFMANN, AND J. REITNER. 1998. Microbial fabric formation in spring mounds ("microbialites") of alkaline salt lakes in the Badain Jaran sand sea, PR China. PALAIOS, 13:581–592.

ARP, G., A. REIMER, AND J. REITNER. 1999. Calcification in cyanobacterial biofilms of alkaline salt lakes. European Journal of Phycology, 34:393–403.

ARP, G., A. REIMER, AND J. REITNER. 2003. Microbialite formation in seawater of increased alkalinity, Satonda Crater Lake, Indonesia. Journal of Sedimentary Research, 73:105–127.

ARP, G., V. THIEL, A. REIMER, W. MICHAELIS, AND J. REITNER. 1999. Biofilm exopolymers control microbialite formation at thermal springs discharging into the alkaline Pyramid Lake, Nevada, USA. Sedimentary Geology, 126:159–176.

AWRAMIK, S. M., AND R. RIDING. 1988. Role of algal eukaryotes in subtidal columnar stromatolite formation. Proceedings of the National Academy of Sciences of the United States of America. 85:1327–1329.

BAO, H., I. J. FAIRCHILD, P. M. WYNN, AND C. SPÖTL. 2009. Stretching the envelope of past surface environments: Neoproterozoic glacial lakes from Svalbard. Science, 323:119–122.

BAO, H. M., J. R. LYONS, AND H. ZHOU. 2008. Triple oxygen isotope evidence for elevated CO_2 levels after a Neoproterozoic glaciation. Nature, 453:504–506.

BATTIN, T. J., L. A. KAPLAN, J. D. NEWBOLD, X. CHENG, AND C. HANSEN. 2003. Effects of current velocity on the nascent architecture of stream microbial biofilms. Applied and Environmental Microbiology, 69:5443–5452.

BAUD, A., S. RICHOZ, AND J. MARCOUX. 2005. Calcimicrobial cap rocks from the basal Triassic units: western Taurus occurrences (SW Turkey). Comptes Rendus Palevol, 4:569–582.

BERELSON, W., F. CORSETTI, C. PEPE-RANNEY, D. HAMMOND, W. BEAUMONT, AND J. SPEAR. 2011. Hot spring siliceous stromatolites from Yellowstone National Park: assessing growth rate and laminae formation. Geobiology, 9:411–424.

BESEMER, K., G. SINGER, R. LIMBERGER, A.-K. CHLUP, G. HOCHEDLINGER, I. HÖDL, C. BARANYI, AND T. J. BATTIN. 2007. Biophysical controls on community succession in stream biofilms. Applied and Environmental Microbiology, 73:4966–4974.

BLACK, M. 1933. The algal sediments of Andros Island, Bahamas. Philosophical Transactions of the Royal Society of London Series B, 222:165–192.

BONTOGNALI, T. R., C. VASCONCELOS, R. J. WARTHMANN, S. M. BERNASCONI, C. DUPRAZ, C. J. STROHMENGER, AND J. A. MCKENZIE. 2010. Dolomite formation within microbial mats in the coastal sabkha of Abu Dhabi (United Arab Emirates). Sedimentology, 57:824–844.

BOSAK, T., J. W. M. BUSH, M. R. FLYNN, B. LIANG, S. ONO, A. P. PETROFF, AND M. S. SIM. 2010. Formation and stability of oxygen-rich bubbles that shape photosynthetic mats. Geobiology, 8:1–11.

BOSAK, T., A. H. KNOLL, AND A. P. PETROFF. 2013. The meaning of stromatolites. Annual Review of Earth and Planetary Sciences, 41:21–44.

BOSAK, T., D. J. G. LAHR, S. B. PRUSS, F. A. MACDONALD, L. DALTON, AND E. MATYS. 2011. Agglutinated tests in post-Sturtian cap carbonates of Namibia and Mongolia. Earth and Planetary Science Letters, 308:29–40.

BOSAK, T., B. LIANG, M. S. SIM,AND A. P. PETROFF.

2009. Morphological record of oxygenic photosynthesis in conical stromatolites. Proceedings of the National Academy of Sciences, 106:10939–10943.

BOSAK, T., B. LIANG, T. D. WU, S. TEMPLER, A. EVANS, H. VALI, J. L. GUERQUIN-KERN, V. KLEPAC-CERAJ, M. SIM, Y. FRIEDMAN, AND J. MUI. 2012. Cyanobacterial diversity and activity in modern conical microbialites. Geobiology, 10:384–401.

BOSAK, T., AND D. K. NEWMAN. 2005. Microbial kinetic controls on calcite morphology in supersaturated solutions. Journal of Sedimentary Research, 75:190–199.

BOSAK, T., V. SOUZA-EGIPSY, F. A. CORSETTI, AND D. K. NEWMAN. 2004. Micrometer-scale porosity as a biosignature in carbonate crusts. Geology, 32:781–784.

BOSAK, T., V. SOUZA-EGIPSY, AND D. K. NEWMAN. 2004. An abiotic model for peloid formation. Geobiology, 2:189–198.

BRISTOW, T. F., M. BONIFACIE, A. DERKOWSKI, J. M. EILER, AND J. P. GROTZINGER. 2011. A hydrothermal origin for isotopically anomalous cap dolostone cements from south China, Nature, 474:68–71.

BROCK, T. D. 1978. Stromatolites: Yellowstone analogues, p. 337-385. *In* T. D. Brock, Thermophilic Organisms and Life at High Temperatures. Springer Series in Microbiology, Springer, New York.

BROWNE, K. M., S. GOLUBIC, AND L. SEONG-JOO. 2000. Shallow marine microbial carbonate deposits, p. 233–249. *In* R. E. Riding and S. M. Awramik (eds.), Microbial sediments. Springer, New York.

BUICK, R. 1992. The antiquity of oxygenic photosynthesis: Evidence from stromatolites in sulphate-deficient Archaean lakes. Science, 255:74–77.

BUICK, R., AND J. S. R. DUNLOP. 1990. Evaporitic sediments of Early Archaean age from the Warrawoona Group, North Pole, Western Australia. Sedimentology, 37:247–277.

BURNE, R. V., AND L. S. MOORE. 1987. Microbialites: organosedimentary deposits of benthic microbial communities. PALAIOS, 2:241–254.

CALVER, C. R., AND M. R. WALTER. 2000. The late Neoproterozoic Grassy Group of King Island, Tasmania: correlation and palaeogeographic significance. Precambrian Research, 100:299–312.

CAMPBELL, K. A. 2006. Hydrocarbon seep and hydrothermal vent paleoenvironments and paleontology: Past developments and future research directions. Palaeogeography, Palaeoclimatology, Palaeoecology, 232:362–407.

CHAFETZ, H. S., AND S. A. GUIDRY. 1999. Bacterial shrubs, crystal shrubs, and ray-crystal shrubs: bacterial vs. abiotic precipitation. Sedimentary Geology, 126:57–74.

CLOUD, P., AND M. SEMIKHATOV. 1969. Proterozoic stromatolite zonation. American Journal of Science, 267:1017–1061.

CLOUD, P. E., JR., L. A. WRIGHT, E. G. WILLIAMS, P. DIEHL, AND M. R. WALTER. 1974. Giant stromatolites and associated vertical tubes from the Upper Proterozoic Noonday Dolomite, Death Valley region, eastern California. Geological Society of America Bulletin, 85:1869–1882.

CORSETTI, F. A., AND J. P. GROTZINGER. 2005. Origin and significance of tube structures in Neoproterozoic post-glacial cap carbonates: Example from Noonday Dolomite, Death Valley, United States. PALAIOS, 20:348–362.

DÉFARGE, C., J. TRICHET, A. MAURIN, AND M. HUCHER. 1994. Kopara in Polynesian atolls: early stages of formation of calcareous stromatolites. Sedimentary Geology, 89:9–23.

DEMICCO, R. V., AND L. A. HARDIE. 1994, Sedimentary Structures and Early Diagenetic Features of Shallow Marine Carbonate Deposits. SEPM Atlas Series Volume 1, SEPM, Tulsa, Oklahoma.

DUPRAZ, C., R. P. REID, O. BRAISSANT,A. W. DECHO, R. S. NORMAN, AND P. T. VISSCHER. 2009. Processes of carbonate precipitation in modern microbial mats. Earth-Science Reviews, 96:141–162.

DUPRAZ, C., AND P. T. VISSCHER. 2005. Microbial lithification in marine stromatolites and hypersaline mats. Trends in Microbiology, 13:429–438.

ECKMAN, J., M. ANDRES, R. MARINELLI, E. BOWLIN, R. REID, R. ASPDEN, AND D. PATERSON. 2008. Wave and sediment dynamics along a shallow subtidal sandy beach inhabited by modern stromatolites. Geobiology, 6:21–32.

FRAISER, M. L., AND F. A. CORSETTI. 2003. Neoproterozoic carbonate shrubs: Interplay of microbial activity and unusual environmental conditions in post-Snowball Earth oceans. PALAIOS, 18:378–387.

FRANKE, U., L. POLERECKY, E. PRECHT, AND M. HUETTEL. 2006. Wave tank study of particulate organic matter degradation in permeable sediments. Limnology and Oceanography, 51:1084–1096.

GEBELEIN, C. D. 1969. Distribution, morphology, and accretion rate of recent subtidal algal stromatolites, Bermuda. Journal of Sedimentary Petrology, 39:49–69.

GEHLING, J. 2000. Environmental interpretation and a sequence stratigraphic framework for the terminal Proterozoic Ediacara Member within the Rawnsley Quartzite, South Australia. Precambrian Research, 100:65–95.

GERDES, G., T. KLENKE, AND N. NOFFKE. 2000. Microbial signatures in peritidal siliciclastic

sediments: a catalogue. Sedimentology, 47:279–308.

GIDDINGS, J. A., AND M. W. WALLACE. 2009. Sedimentology and C-isotope geochemistry of the 'Sturtian' cap carbonate, South Australia. Sedimentary Geology, 216:1–14.

GINSBURG, R. N., AND H. A. LOWENSTAM. 1958. The influence of marine bottom communities on the depositional environment of sediments. The Journal of Geology, 66:310–318.

GODILLOT, R., B. CAUSSADE, T. AMEZIANE, AND J. CAPBLANCQ. 2001. Interplay between turbulence and periphyton in rough open-channel flow. Journal of Hydraulic Research, 39:227–239.

GOLUBIC, S. 1982. Stromatolites, fossil and recent: a case history, p. 313–326. *In* P. Westbroek and E. W. De Jong (eds.), Biomineralization and Biological Metal Accumulation. D. Reidel Publishing Company, Dordrecht.

GRABA, M., F. Y. MOULIN, S. BOULÊTREAU, F. GARABÉTIAN, A. KETTAB, O. EIFF, J. M. SANCHEZ-PÉREZ, AND S. SAUVAGE. 2010. Effect of near-bed turbulence on chronic detachment of epilithic biofilm: Experimental and modeling approaches. Water Resources Research, 46:W11531. doi: 10.1029/2009WR008679.

GRABA, M., S. SAUVAGE, F. Y. MOULIN, G. URREA, S. SABATER, AND J. M. SANCHEZ-PÉREZ. 2013. Interaction between local hydrodynamics and algal community in epilithic biofilm. Water Research, 47:2153–2163.

GREGG, J. M., AND K. L. SHELTON. 1990. Dolomitization and dolomite neomorphism in the back reef facies of the Bonneterre and Davis formations (Cambrian), southeastern Missouri. Journal of Sedimentary Research, 60:549–562.

GREY, K., AND A. M. THORNE. 1985. Biostratigraphic significance of stromatolites in upward shallowing sequences of the early Proterozoic Duck Creek Dolomite, Western Australia. Precambrian Research, 29:183–206.

GROTZINGER, J. P., AND A. H. KNOLL. 1999. Stromatolites in Precambrian carbonates: Evolutionary mileposts or environmental dipsticks? Annual Review of Earth and Planetary Sciences, 27:313–358.

HALVERSON, G. P., A. C. MALOOF, AND P. F. HOFFMAN. 2004. The Marinoan glaciation (Neoproterozoic) in northeast Svalbard. Basin Research, 16:297–324.

HARWOOD, C. L., AND D. Y. SUMNER. 2011. Microbialites of the Neoproterozoic Beck Spring Dolomite, Southern California. Sedimentology, 58:1648–1673.

HEGENBERGER, W. 1987. Gas escape structures in Precambrian peritidal carbonate rocks. Communications of the Geological Survey of South West Africa/Namibia, 3:49–55.

HIGGINS, J. A., W. W. FISCHER, AND D. P. SCHRAG. 2009. Oxygenation of the ocean and sediments: Consequences for the seafloor carbonate factory. Earth and Planetary Science Letters, 284:25–33.

HIGGINS, J. A., AND D. P. SCHRAG. 2003. Aftermath of a Snowball Earth. Geochemistry, Geophysics, Geosystems, 4:1028. doi: 10.1029/2002GC000403.

HOFFMAN, P. 1974. Shallow and deepwater stromatolites in lower Proterozoic platform-to-basin facies change, Great Slave Lake, Canada. American Association of Petroleum Geologists Bulletin, 58:865–867.

HOFFMAN, P. F. 1976. Stromatolite morphogenesis in Shark Bay, Western Australia, p. 261–272. *In* M. R. Walter (ed.), Stromatolites. Elsevier, Amsterdam.

HOFFMAN, P. F. 2011. Strange bedfellows: glacial diamictite and cap carbonate from the Marinoan (635 Ma) glaciation in Namibia. Sedimentology, 58:57–119.

HOFFMAN, P. F., AND G. P. HALVERSON. 2008. Otavi Group of the western Northern Platform, the Eastern Kaoko Zone and the western Northern Margin Zone, p. 13.69–13.136. *In* R. M. Miller (ed.), The Geology of Namibia, Volume 2. Handbook of the Geological Survey of Namibia, Windhoek.

HOFFMAN, P. F., AND G. P. HALVERSON. 2011. Neoproterozoic glacial record in the Mackenzie Mountains, northern Canadian Cordillera, p. 397–412. *In* E. Arnaud, G. P. Halverson, and G. Shields-Zhou (eds.), The Geological Record of Neoproterozoic Glaciations. The Geological Society of London Memoirs 36, London.

HOFFMAN, P. F., G. P. HALVERSON, E. W. DOMACK, J. M. HUSSON, J. A. HIGGINS, AND D. P. SCHRAG. 2007. Are basal Ediacaran (635 Ma) post-glacial "cap dolostones" diachronous? Earth and Planetary Science Letters, 258:114–131.

HOFFMAN, P. F., A. J. KAUFMAN, G. P. HALVERSON, AND D. P. SCHRAG. 1998. A Neoproterozoic Snowball Earth. Science, 281:1342–1346.

HOFFMAN, P. F., AND F. A. MACDONALD. 2010. Sheet-crack cements and early regression in Marinoan (635 Ma) cap dolostones: Regional benchmarks of vanishing ice-sheets? Earth and Planetary Science Letters, 300:374–384.

HOFFMAN, P. F., AND D. P. SCHRAG. 2002. The Snowball Earth hypothesis: testing the limits of global change. Terra Nova, 14:129–155.

HOFMANN, H. 1975. Stratiform Precambrian stromatolites, Belcher Islands, Canada; relations between silicified microfossils and microstructure. American Journal of Science, 275:1121–1132.

HOFMANN, H. J. 2000. Archean stromatolites as microbial archives, p. 315–327. *In* R. E. Riding and S. M. Awramik (eds.), Microbial Sediments.

Springer, Berlin Heidelberg.

HORODYSKI, R. J. 1975. Stromatolites of the lower Missoula Group (Middle Proterozoic), Belt Supergroup, Glacier National Park, Montana. Precambrian Research, 2:215–254.

HORODYSKI, R. J., B. BLOESER, AND S. VONDER HAAR. 1977. Laminated algal mats from a coastal lagoon, Laguna Mormona, Baja California, Mexico. Journal of Sedimentary Research, 47:680–696.

HUETTEL, M., AND G. GUST. 1992. Impact of bioroughness on interfacial solute exchange in permeable sediments. Marine Ecology Progress Series, 89:253–267.

HUETTEL, M., W. ZIEBIS, S. FORSTER, AND G. LUTHER. 1998. Advective transport affecting metal and nutrient distributions and interfacial fluxes in permeable sediments. Geochimica Et Cosmochimica Acta, 62:613–631.

JAHNERT, R. J., AND L. B. COLLINS. 2012. Characteristics, distribution and morphogenesis of subtidal microbial systems in Shark Bay, Australia. Marine Geology, 303:115–136.

JAMES, N. P., G. M. NARBONNE, AND T. K. KYSER. 2001. Late Neoproterozoic cap carbonates: Mackenzie Mountains, northwestern Canada: precipitation and global glacial meltdown. Canadian Journal of Earth Sciences, 38:1229–1262.

JEROLMACK, D. J., AND D. MOHRIG. 2005. Formation of Precambrian sediment ripples: Arising from P.A. Allen, P.F. Hoffman. Nature, 433:123–127.

JIANG, G., M. J. KENNEDY, AND N. CHRISTIE-BLICK. 2003. Stable isotopic evidence for methane seeps in Neoproterozoic postglacial cap carbonates. Nature, 426:822–826.

JIANG, G., M. J. KENNEDY, N. CHRISTIE-BLICK, H. WU, AND S. ZHANG. 2006. Stratigraphy, sedimentary structures, and textures of the late Neoproterozoic Doushantuo cap carbonate in South China. Journal of Sedimentary Research, 76:978–995.

JOHNSON, D. B., AND K. B. HALLBERG. 2003. The microbiology of acidic mine waters. Research in Microbiology, 154:466–473.

JONES, B., AND R. W. RENAUT. 1996. Morphology and growth of aragonite crystals in hot-spring travertines at Lake Bogoria, Kenya Rift Valley. Sedimentology, 43:323–340.

JONES, B., AND R. W. RENAUT. 2008. Cyclic development of large, complex, calcite dendrite crystals in the Clinton travertine, Interior British Columbia, Canada. Sedimentary Geology, 203:17–35.

KAH, L. C., AND A. H. KNOLL. 1996. Microbenthic distribution of Proterozoic tidal flats: Environmental and taphonomic considerations. Geology, 24:79–82.

KASEMANN, S. A., C. J. HAWKESWORTH, A. R. PRAVE, A. E. FALLICK, AND P. N. PEARSON. 2005. Boron and calcium isotope composition in Neoproterozoic carbonate rocks from Namibia: evidence for extreme environmental change. Earth and Planetary Science Letters, 231:73–86.

KASEMANN, S. A., A. R. PRAVE, A. E. FALLICK, C. J. HAWKESWORTH, AND K.-H. HOFFMANN. 2010. Neoproterozoic ice ages, boron isotopes, and ocean acidification: Implications for a snowball Earth. Geology, 38:775–778.

KAŹMIERCZAK, J., M. L. COLEMAN, M. GRUSZCZYNSKI, AND S. KEMPE. 1996. Cyanobacterial key to the genesis of micritic and peloidal limestones in ancient seas. Acta Palaeontologica Polonica, 41:319–338.

KENNEDY, M. J. 1996. Stratigraphy, sedimentology, and isotope geochemistry of Australian Neoproterozoic postglacial cap dolostones: deglaciation, $\delta^{13}C$ excursions, and carbonate precipitation. Journal of Sedimentary Research, 66:1050–1064.

KENNEDY, M. J., AND N. CHRISTIE-BLICK. 2011. Condensation origin for Neoproterozoic cap carbonates during deglaciation. Geology, 39:319–322.

KENNEDY, M. J., N. CHRISTIE-BLICK, AND L. E. SOHL. 2001. Are Proterozoic cap carbonates and isotopic excursions a record of gas hydrate destabilization following Earth's coldest intervals? Geology, 29:443–446.

KILNER, B., C. NIOCAILL, AND M. BRASIER. 2005. Low-latitude glaciation in the Neoproterozoic of Oman. Geology, 33:413–416.

KNOLL, A. H., AND M. A. SEMIKHATOV. 1998. The genesis and time distribution of two distinctive Proterozoic stromatolite microstructures. PALAIOS, 13:408–422.

LABIOD, C., R. GODILLOT, AND B. CAUSSADE. 2007. The relationship between stream periphyton dynamics and near-bed turbulence in rough open-channel flow. Ecological Modelling, 209:78–96.

LAMB, M. P., W. W. FISCHER, T. D. RAUB, J. T. PERRON, AND P. M. MYROW. 2012. Origin of giant wave ripples in snowball Earth cap carbonate. Geology, 40:827–830.

LE BER, E., D. LE HERON, G. WINTERLEITNER, D. BOSENCE, B. VINING, AND F. KAMONA. 2013. Microbialite recovery in the aftermath of the Sturtian glaciation: Insights from the Rasthof Formation, Namibia. Sedimentary Geology, in press.

LOGAN, B. W. 1961. Cryptozoon and associate stromatolites from the Recent, Shark Bay, Western Australia. Journal of Geology, 69:517–533.

LOGAN, B. W., R. REZAK, AND R. N. GINSBURG. 1964. Classification and environmental significance of algal stromatolites. Journal of Geology, 72:68–83.

MACDONALD, F. A., D. S. JONES, AND D. P. SCHRAG. 2009a. Stratigraphic and tectonic implications of a

new glacial diamictite-cap carbonate couplet in southwestern Mongolia. Geology, 37:123–126.

MACDONALD, F. A., W. C. MCCLELLAND, D. P. SCHRAG, AND W. P. MACDONALD. 2009b. Neoproterozoic glaciation on a carbonate platform margin in Arctic Alaska and the origin of the North Slope subterrane. Geological Society of America Bulletin 121:448–473.

MACDONALD, F. A., J. V. STRAUSS, C. V. ROSE, F. O. DUDÁS, AND D. P. SCHRAG. 2010. Stratigraphy of the Port Nolloth Group of Namibia and South Africa and implications for the age of Neoproterozoic iron formations. American Journal of Science, 310:862–888.

MARIOTTI, G., AND S. FAGHERAZZI. 2012. Modeling the effect of tides and waves on benthic biofilms. Journal of Geophysical Research: Biogeosciences (2005-2012). 117:G04010.

MARTÍN, J. M., J. C. BRAGA, AND R. RIDING. 1997. Late Miocene Halimeda alga-microbial segment reefs in the marginal Mediterranean Sorbas Basin, Spain. Sedimentology, 44:441–456.

MATA, S. A., C. L. HARWOOD, F. A. CORSETTI, N. J. STORK, K. EILERS, W. M. BERELSON, AND J. R. SPEAR. 2012. Influence of gas production and filament orientation on stromatolite microfabric. PALAIOS, 27:206–219.

MILLIMAN, J. D. 1993. Production and accumulation of calcium carbonate in the ocean: Budget of a nonsteady state. Global Biogeochemical Cycles, 7:927–957.

MONTY, C. L. V. 1976. The origin and development of cryptalgal fabrics, p. 193–250. *In* M. R. Walter (ed.), Stromatolites. Elsevier, Amsterdam.

MORSE, J. W., R. S. ARVIDSON, AND A. LUTTGE. 2007. Calcium carbonate formation and dissolution. Chemical Reviews-Columbus, 107:342–381.

NEUMANN, A. C., C. D. GEBELEIN, AND T. P. SCOFFIN. 1970. The composition, structure and erodability of subtidal mats, Abaco, Bahamas. Journal of Sedimentary Petrology, 40:274–297.

NIEDERBERGER, T. D., N. PERREAULT, J. R. LAWRENCE, L. J. NADEAU, R. E. MIELKE, C. W. GREER, D. T. ANDERSEN, AND L. G. WHYTE. 2009. Novel sulfur-oxidizing streamers thriving in perennial cold saline springs of the Canadian high Arctic. Environmental Microbiology, 11:616–629.

NIKORA, V., D. GORING, AND B. BIGGS. 1997. On stream periphyton-turbulence interactions. New Zealand Journal of Marine and Freshwater Research, 31:435–448.

NOFFKE, N. 2010. Geobiology: Microbial Mats in Sandy Deposits from the Archean Era to Today. Springer, Heidelberg.

NOFFKE, N., G. GERDES, T. KLENKE, AND W. E. KRUMBEIN. 2001. Microbially induced sedimentary structures—A new category within the classification of primary sedimentary structures: perspectives. Journal of Sedimentary Research, 71:649–656.

OKUMURA, T., C. TAKASHIMA, F. SHIRAISHI, AKMALUDDIN, AND A. KANO. 2012. Textural transition in an aragonite travertine formed under various flow conditions at Pancuran Pitu, Central Java, Indonesia. Sedimentary Geology, 265–266:195–209.

PATERSON, D. M. 1997. Biological mediation of sediment erodibility: ecology and physical dynamics, p. 215-229. *In* N. Burt, R. Parker and J. Watts (eds.), Cohesive Sediments. John Wiley and Sons, Hoboken, New Jersey.

PAYNE, J. L., A. V. TURCHYN, A. PAYTAN, D. J. DEPAOLO, D. J. LEHRMANN, M. YU, AND J. WEI. 2010. Calcium isotope constraints on the end-Permian mass extinction. Proceedings of the National Academy of Sciences, 107:8543–8548.

PENTECOST, A. 1990. The formation of travertine shrubs: Mammoth Hot Springs, Wyoming. Geological Magazine, 127:159–168.

PERRI, E., M. E. TUCKER, AND A. SPADAFORA. 2012. Carbonate organo-mineral micro- and ultrastructures in sub-fossil stromatolites: Marion Lake, South Australia. Geobiology, 10:105–117.

PETROFF, A. P., D. H. ROTHMAN, N. J. BEUKES, AND T. BOSAK. in press. Biofilm growth and fossil form. Physical Review.

PETROFF, A. P., M. S. SIM, A. MASLOV, M. KRUPENIN, D. H. ROTHMAN, AND T. BOSAK. 2010. Biophysical basis for the geometry of conical stromatolites. Proceedings of the National Academy of Sciences, 107:9956–9961.

PETRYSHYN, V. A., AND F. A. CORSETTI. 2011. Analysis of growth directions of columnar stromatolites from Walker Lake, western Nevada. Geobiology, 9:425–435.

PLAYFORD, P. E. 1980. Environmental controls on the morphology of modern stromatolites at Hamelin Pool, Western Australia. Western Australia Geological Survey Annual Report for 1979. Benbow Publishing Co., Perth, Western Australia, p. 73–77

PLAYFORD, P. E., AND A. E. COCKBAIN. 1976. Modern algal stromatolites at Hamelin Pool, a hypersaline barred basin in Shark Bay, Western Australia, p. 389–411. *In* M. R. Walter (ed.), Stromatolites. Elsevier, Amsterdam.

PRECHT, E., U. FRANKE, L. POLERECKY, AND M. HUETTEL. 2004. Oxygen dynamics in permeable sediments with wave-driven pore water exchange. Limnology and Oceanography, 49:693–705.

PRECHT, E., AND M. HUETTEL. 2003. Advective pore-water exchange driven by surface gravity waves and its ecological implications. Limnology and Oceanography, 48:1674–1684.

PRUSS, S. B., T. BOSAK, T., F. A. MACDONALD, M. MCLANE, AND P. F. HOFFMAN. 2010. Microbial

facies in a Sturtian cap carbonate, the Rasthof Formation, Otavi Group, northern Namibia. Precambrian Research, 181:187–198.

RAABEN, M. 2006. Dimensional parameters of columnar stromatolites as a result of stromatolite ecosystem evolution. Stratigraphy and Geological Correlation. 14:150–163.

RADU, A., J. VROUWENVELDER, M. VAN LOOSDRECHT, AND C. PICIOREANU. 2012. Effect of flow velocity, substrate concentration and hydraulic cleaning on biofouling of reverse osmosis feed channels. Chemical Engineering Journal, 188:30–39.

REID, R. P. 1987. Nonskeletal peloidal precipitates in upper Triassic reefs, Yukon Territory (Canada). Journal of Sedimentary Research, 57:893–900.

REID, R. P., N. P. JAMES, I. G. MACINTYRE, C. P. DUPRAZ, AND R. V. BURNE. 2003. Shark Bay stromatolites: Microfabrics and reinterpretation of origins. Facies, 49:299–324.

REID, R. P., P. T. VISSCHER, A. W. DECHO, J. F. STOLZ, B. M. BEBOUT, C. DUPRAZ, L. G. MACINTYRE, H. W. PAERL, J. L. PINCKNEY, L. PRUFERT-BEBOUT, T. F. STEPPE, AND D. J. DESMARAIS. 2000. The role of microbes in accretion, lamination and early lithification of modern marine stromatolites. Nature, 406:989–992.

RIDING, R. 2000. Microbial carbonates: the geological record of calcified bacterial-algal mats and biofilms. Sedimentology, 47:179–214.

RIDING, R., AND S. TOMÁS. 2006. Stromatolite reef crusts, Early Cretaceous, Spain: bacterial origin of in situ-precipitated peloid microspar? Sedimentology, 53:23–34.

ROONEY, A. D., F. A. MACDONALD, F. O. DUDÁS, C. HALLMANN, J. V. STRAUSS, AND D. SELBY. in review. Weathering the Snowball.

SAMI, T. T., AND N. P. JAMES. 1994. Peritidal carbonate platform growth and cyclicity in an early Proterozoic foreland basin, upper Pethei Group, northwest Canada. Journal of Sedimentary Research, 64:111–131.

SANTOS, I. R., B. D. EYRE, AND M. HUETTEL. 2012. The driving forces of porewater and groundwater flow in permeable coastal sediments: A review. Estuarine, Coastal and Shelf Science. 98:1–15.

SCHIEBER, J., P. K. BOSE, P. G. ERIKSSON, S. BANERJEE, S. SARKAR, W. ALTERMANN, AND O. CATUNEANU. 2007. Atlas of Microbial Mat Features Preserved Within The Siliciclastic Rock Record. Atlases in Geoscience Volume 2, Elsevier, Amsterdam.

SCHMIDT, P. W., G. E. WILLIAMS, AND M. O. MCWILLIAMS. 2009. Palaeomagnetism and magnetic anisotropy of late Neoproterozoic strata, South Australia: Implications for the palaeolatitude of late Cryogenian glaciation, cap carbonate and the Ediacaran System. Precambrian Research, 174:35–52.

SCHOPF, J. W. 2006. Fossil evidence of Archaean life. Philosophical Transactions of the Royal Society of London, Series B, 361:869–885.

SCHRÖDER, S., N. J. BEUKES, AND D. Y. SUMNER. 2009. Microbialite-sediment interactions on the slope of the Campbellrand carbonate platform (Neoarchean, South Africa). Precambrian Research, 169:68–79.

SCOFFIN, T. P. 1970. The trapping and binding of subtidal carbonate sediments by marine vegetation in Bimini Lagoon, Bahamas. Journal of Sedimentary Research, 40:249–273.

SEMIKHATOV, M., C. GEBELEIN, P. CLOUD, S. AWRAMIK, AND W. BENMORE. 1979. Stromatolite morphogenesis-progress and problems. Canadian Journal of Earth Sciences, 16:992–1015.

SEMIKHATOV, M., AND M. RAABEN. 1996. Dynamics of the global diversity of Proterozoic stromatolites. Article II: Africa, Australia, North America, and general synthesis. Stratigraphy and Geological Correlation, 4:24–50.

SEONG-JOO, L., K. M. BROWNE, AND S. GOLUBIC. 2000. On stromatolite lamination, p. 16–24. *In* R. E. Riding and S. M. Awramik (eds.), Microbial Sediments. Springer, Heidelberg.

SEONG-JOO, L., AND S. GOLUBIC. 2000. Biological and mineral components of an ancient stromatolite: Gaoyuzhuang Formation, Mesoproterozoic of China, p. 91–102. *In* J. P. Grotzinger and N. P. James (eds.), Carbonate Sedimentation and Diagenesis in the Evolving Precambrian World. SEPM Special Publication Volume 67, SEPM, Tulsa, Oklahoma.

SHIELDS, G. A. 2005. Neoproterozoic cap carbonates: a critical appraisal of existing models and the plumeworld hypothesis. Terra Nova, 17:299–310.

SIM, M. S., B. LIANG, A. P. PETROFF, A. EVANS, V. KLEPAC-CERAJ, D. T. FLANNERY, M. R. WALTER, AND T. BOSAK. 2012. Oxygen-dependent morphogenesis of modern clumped photosynthetic mats and implications for the Archean stromatolite record. Geosciences, 2:235–259.

SIMONSON, B. M., AND K. E. CARNEY. 1999. Roll-up structures; evidence of in situ microbial mats in late Archean deep shelf environments. PALAIOS, 14:13–24.

SPADAFORA, A., E. PERRI, J. A. MCKENZIE, AND C. VASCONCELOS. 2010. Microbial biomineralization processes forming modern Ca:Mg carbonate stromatolites. Sedimentology, 57:27–40.

SPRACHTA, S., G. CAMOIN, S. GOLUBIC, AND T. LE CAMPION. 2001. Microbialites in a modern lagoonal environment: nature and distribution, Tikehau atoll (French Polynesia). Palaeogeography, Palaeoclimatology, Palaeoecology, 175:103–124.

SUN, S., AND V. WRIGHT. 1989. Peloidal fabrics in Upper Jurassic reefal limestones, Weald Basin, southern England. Sedimentary Geology, 65:165–

181.

TICE, M. M., D. C. THORNTON, M. C. POPE, T. D. OLSZEWSKI., AND J. GONG. 2011. Archean microbial mat communities. Annual Review of Earth and Planetary Sciences, 39:297–319.

TRIBOVILLARD, N., A. TRENTESAUX, J. TRICHET, AND C. DÉFARGE. 2000. A Jurassic counterpart for modern kopara of the Pacific atolls: lagoonal, organic matter-rich, laminated carbonate of Orbagnoux (Jura Mountains, France). Palaeogeography, Palaeoclimatology, Palaeoecology, 156:277–288.

TRICHET, J., AND C. DÉFARGE. 1995. Non-biologically supported organomineralization. Bulletin of the Oceanographic Institute, Monaco. 14:203–236.

TRICHET, J., C. DÉFARGE, J. TRIBBLE, G. TRIBBLE, AND F. SANSONe. 2001. Christmas Island lagoonal lakes, models for the deposition of carbonate-evaporite-organic laminated sediments. Sedimentary Geology, 140:177–189.

TRINDADE, R., E. FONT, M. D'AGRELLA-FILHO, A. NOGUEIRA, AND C. RICCOMINI. 2003. Low-latitude and multiple geomagnetic reversals in the Neoproterozoic Puga cap carbonate, Amazon craton. Terra Nova, 15:441–446.

TURNER, E. C., N. P. JAMES, AND G. M. NARBONNE. 2000. Taphonomic control on microstructure in Early Neoproterozoic reefal stromatolites and thrombolites. PALAIOS, 15:87–111.

UEHLINGER, U., H. BÜHRER, AND P. REICHERT. 1996. Periphyton dynamics in a floodprone prealpine river: evaluation of significant processes by modelling. Freshwater Biology, 36:249–263.

VASCONCELOS, C., R. WARTHMANN, J. A. MCKENZIE, P. T. VISSCHER, A. G. BITTERMANN, AND Y. VAN LITH. 2006. Lithifying microbial mats in Lagoa Vermelha, Brazil: Modern Precambrian relics? Sedimentary Geology, 185:175–183.

VISSCHER, P. T., R. P. REID, AND B. M. BEBOUT. 2000. Microscale observations of sulfate reduction: Correlation of microbial activity with lithified micritic laminae in modern marine stromatolites. Geology, 28:919–922.

WALTER, M., AND G. HEYS. 1985. Links between the rise of the Metazoa and the decline of stromatolites. Precambrian Research, 29:149–174.

WALTER, M. R., J. BAULD, AND T. D. BROCK. 1976. Microbiology and morphogenesis of columnar stromatolites (Conophyton, Vacerrilla) from hot springs in Yellowstone National Park, p. 273–310. *In* M. R. Walter (ed.), Stromatolites. Elsevier, Amsterdam.

WRIGHT, L. A., E. G. WILLIAMS, AND P. CLOUD. 1978. Algal and cryptalgal structures and platform environments of the late pre-Phanerozoic Noonday Dolomite, eastern California. Geological Society of America Bulletin, 89:321–333.

XIAO, S., H. BAO, H. WANG, A. J. KAUFMAN, C. ZHOU, G. LI, X. YUAN, AND H. LING. 2004. The Neoproterozoic Quruqtagh Group in eastern Chinese Tianshan: evidence for a post-Marinoan glaciation. Precambrian Research, 130:1–26.